BM5 / C. Woodsmall Copy No.

NATIONAL AERONAUTICS AND SPACE ADMINISTRATION

NASA PROGRAM APOLLO WORKING PAPER NO. 1320

AN ANALYSIS OF PARACHUTE HEATING IN MANNED SPACECRAFT LAUNCH ABORT SITUATIONS

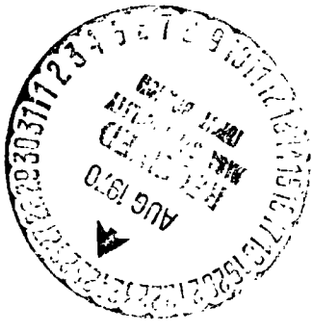

MANNED SPACECRAFT CENTER
HOUSTON, TEXAS

June 21, 1967

NASA PROGRAM APOLLO WORKING PAPER NO. 1320

AN ANALYSIS OF PARACHUTE HEATING IN MANNED SPACECRAFT LAUNCH ABORT SITUATIONS

PREPARED BY

Noel C. Willis, Jr.
Environmental Control Systems Branch

Edward T. Chimenti
Thermal Technology Branch

AUTHORIZED FOR DISTRIBUTION

for Maxime A. Faget
Director of Engineering and Development

NATIONAL AERONAUTICS AND SPACE ADMINISTRATION
MANNED SPACECRAFT CENTER
HOUSTON, TEXAS
June 21, 1967

CONTENTS

FIGURES

AN ANALYSIS OF PARACHUTE HEATING IN MANNED SPACECRAFT LAUNCH ABORT SITUATIONS

By Noel C. Willis, Jr. and
Edward T. Chimenti

SUMMARY

To insure safety of a spacecraft flight crew while the launch vehicle is either on the pad or in powered flight, launch escape systems have been developed to rapidly accelerate the spacecraft away from a malfunctioning booster, and subsequently lower it to earth by parachute. In the unlikely event that a malfunction occurred which indicated the possibility of a booster explosion, the abort sequence would be initiated. If, in fact, the booster did explode, one possible source of danger to the flight crew would be the weakening or melting of the launch escape system parachutes by the radiant heat from the fireball.

In this study, approximate techniques have been developed to determine the effect of a fireball on the temperature history of launch escape system parachutes for various abort conditions. Both drogue and main parachutes have been considered.

Results have been obtained for several Apollo abort conditions in the presence of Saturn V explosions. A semiempirical relation for radiative heating due to the fireball is assumed as the heat input function. These results indicate no parachute failures due to heating for nominal abort conditions, based on the maximum allowable main parachute-temperature criteria of 400° F for a three-parachute descent.

For pad abort trajectories with initial pitch and pitch rates corresponding to the uprange limits of the proposed Apollo emergency destruct system, the main parachutes could fail for certain explosion times. These failures could be prevented by a forced detonation of the booster soon after abort such that the heat pulse would be spent prior to parachute deployment. The initial conditions which would cause this failure do not correspond to a defined Saturn V failure on the pad but are included to illustrate possible problems for off-nominal cases.

INTRODUCTION

In the event an emergency condition exists during a manned spaceflight mission when the launch vehicle is either on the launch pad or in powered flight, the launch escape system rockets will lift the spacecraft away from the potentially hazardous booster. The spacecraft would then be lowered to earth by its parachutes. In order to properly assess the overall safety of this abort mode, one must consider the remote possibility of a launch vehicle explosion and the effect of the radiant heat from the resulting fireball on the structural integrity of the parachutes. The purpose of the study is to develop a method for analyzing the cooling processes taking place during the descent of a parachute so that its temperature history may be calculated.

The thermal analysis accounts for cooling mechanisms due to flow through the parachute material, flow along the surface and surface radiation. Different approximations for these cooling terms are developed for the different configurations of the parachute including reefed inflation, opening, and full inflation.

To illustrate application of the analysis to a specific problem, temperature histories of the parachutes have been calculated for several Apollo abort trajectories in the presence of a Saturn V explosion. Heating rates and time dependence used to represent a Saturn V explosion were estimated semiempirically from observations of other booster explosions.

SYMBOLS

A_c area of drogue chute opening

A_s area of drogue chute slots

C rate of heat removal due to cooling processes

c_p nylon specific heat

h heat transfer coefficient

h_n heat transfer coefficient due to flow through the parachute material

h_t heat transfer coefficient due to tangential flow

K	experimental constant (see eq. (8))
k	thermal conductivity of nylon
l	characteristic length
m	experimental constant (see eq. (8))
N_u	Nusselt number
P_r	Prandtl number
Q	incident heating rate on parachute due to booster explosion
R_e	Reynolds number
T_a	temperature of ambient air
T_d	drogue parachute temperature
T_p	main parachute temperature
T_{sa}	radiation source temperature of the atmosphere
T_{sg}	radiation source temperature of the ground
t_c	time after chute deployment
V	parachute descent velocity
V_E	flow velocity on external parachute surface
V_I	flow velocity on internal parachute surface
α	absorptivity of parachute nylon, 0.229
ε	emissivity of parachute nylon, 0.73
ρ	mass density of nylon
$\rho\tau$	mass per unit area of nylon, 1.1 oz/yd^2

σ Stefan-Boltzman constant, 0.48×10^{-12} $\frac{\text{Btu}}{\text{ft}^4/\text{sec}/^\circ\text{F}}$

τ parachute thickness

MAIN PARACHUTE DESCRIPTION AND ANALYSIS

Parachute Configuration

In order to determine the temperature history of a parachute, one must consider the air flow patterns around and through the parachute material for its various configurations during opening and steady-state descent. The deployment sequence for the Apollo parachutes described below is typical for parachutes used for spacecraft soft landing. The sequence is illustrated in figure 1.

The spacecraft descent is stabilized by drogue parachutes (see fig. 1(a)). The drogues are released and pilot parachutes are deployed to extract the main parachutes (fig. 1(b)). The time of deployment of the pilot parachutes is to be called the beginning of main chute deployment. Approximately 2 seconds after the pilot chutes are deployed, the main parachutes have been pulled out of the spacecraft to the limit of their shroud lines (fig. 1(c)). This event is called line stretch and is the first time the main parachutes are exposed to possible heating. Less than 1 second after line stretch, the main parachutes are inflated in a reefed condition (fig. 1(d)). The reefing lines are cut and the full opening process begins about 8 seconds after line stretch. The parachutes are fully inflated and a constant velocity descent begins 2 or 3 seconds later (fig. 1(e)).

For the purpose of heating analysis of the Apollo parachutes, the descent has been divided into three stages: (a) from line stretch to disreefing or reefed inflation ($2 \leq t_c < 10$ sec), (b) the opening period from disreefing to beginning of steady-state descent ($10 \leq t_c \leq 12.5$ sec), and (c) steady-stated descent $\left(t_c > 12.5 \text{ sec}\right)$. Since the flow patterns for these stages are different, a cooling term must be determined for each. A similar breakdown of the descent stages could be made for other parachutes.

The Apollo main parachutes are of the ringsail type. Figure 2 illustrates the details of the individual panel construction. The load on the panel is supported by the parachute sail material (1.1-oz/yd^2 nylon) and the parachute tape material.

The load-carrying capability of each material is dependent upon its temperature. Because of the different densities and porosities of these two materials, their temperature histories will differ, and they will be analyzed separately.

Heating Analysis

The temperature history of the parachutes is determined by considering the heat-balance equation for the material. The rate of increase of the heat stored in the material is equated to the difference between the rate of heat absorption and the rate of heat removal. The resulting relation is solved for temperature as a function of time for a given trajectory and time of booster explosion.

The general equation governing the parachute temperature $\left(T_p\right)$ as a function of time (t) is

$$c_p \rho \tau \frac{dT_p}{dt_c} = \alpha Q - C \tag{1}$$

where ρ is the material density, c_p its specific heat, and τ its thickness. The term αQ is the incident radiative heating rate from the booster explosion multiplied by the material absorptivity and C is the cooling rate for the particular parachute configuration.

The central objective of this analysis is to develop a suitable approximation for this cooling rate. The cooling C must be estimated in all three stages of descent for both the parachute sail material and the tape. Because the cooling process during opening depends on the transition from full reefed inflation to steady-state descent, the cooling terms for these two stages will be discussed first.

Stage From Line Stretch to Disreefing $\left(t_c = 2 \text{ sec to } t_c = 10 \text{ sec}\right)$

Since full reefed inflation is achieved approximately 3 seconds after deployment, the heating during this stage is analyzed based on the configuration shown in figure 3. The cooling due to an airflow past the surface is predicted by using equations applicable to turbulent flow over a flat plate. Calculation of the Reynolds number based on the air velocity at the parachute surface and the length of the individual sails indicates turbulent flow does exist. The nylon is cooled by flow at the free stream velocity over both the internal and external surfaces.

The Reynolds number per foot at steady descent conditions (30 fps) is approximately 200 000. Prior to steady descent the velocity, and hence the Reynolds number, is considerably higher. Motion pictures of the Apollo parachutes indicate a random flutter of the individual sails, even of steady descent. This motion causes an unsteady movement of the air normal to the surface, thereby inducing turbulence or a motion equivalent to turbulence in its effect on local heat transfer. Laminar flow may possibly exist on the leading sail; however, it is reinforced and will not be the critically loaded sail.

The configuration of the parachute must be considered to determine the proper length to be used in the flat plate equations. The width of the rings in the fully inflated section is 3 feet. However, the ring-slot section has not been inflated, and flow is effectively parallel to both sides of the surface with very little flow through the slots. Even though the individual rings are only 3 feet across, it is a more realistic (and conservative) approximation to treat this entire section as a flat plate of 25.3 feet in length. Since it is of interest to determine the maximum temperature (minimum cooling), the heat transfer coefficient for this descent stage is equated to the local heat transfer coefficient at a point 25.3 feet from the leading edge of a flat plate. The heat transfer coefficient is calculated from the following relation based on a 1/7-power velocity distribution for turbulent flow

$$N_u = \frac{h_t l}{k} = 0.0292 \left(R_e\right)^{0.8} \left(P_r\right)^{1/3} \tag{2}$$

The heat transfer coefficient due to flow parallel to the material will be referred to as the tangential heat transfer coefficient h_t to distinguish it from the heat transfer coefficient for flow through the material h_n. The latter is considered negligible in this case. The normal heat transfer coefficient will become significant in the fully inflated configuration when a pressure differential exists across the nylon sufficient to cause flow through the material. Additional cooling from radiation is also considered for both internal and external surfaces. The radiative term is

$$2\varepsilon\sigma\left(T_p^{\,4} - T_{sa}^{\,4}\right) \tag{3}$$

where ε and σ are, respectively, the nylon emissivity and the Stefan-Boltzman constant. The air source temperature for radiation is T_{sa} and the ambient air temperature is T_a.

Therefore, the total cooling term during this stage is

$$C = h_t\left(T_p - T_a\right) + 2\varepsilon\sigma\left(T_p^4 - T_{sa}^4\right) \tag{4}$$

Stage of Steady-State Descent $\left(t_c > 12.5 \text{ sec}\right)$

During steady-state descent, an additional cooling effect is obtained from airflow through the parachute sail material. This effect is accounted for by the use of a second heat transfer coefficient h_n. This normal coefficient has been correlated as a function of parachute temperature based on unpublished experimental data obtained for the Gemini Program (fig. 4). For a detailed discussion of the derivation of the temperature dependence of h_n, see the appendix. The cooling contribution due to flow through the sail material is

$$h_n\left(T_p - T_a\right) \tag{5}$$

Radiative cooling is calculated for the inner surface using the ground source temperature T_{sg} while the air source temperature T_{sa} is used for the outer surface. The resulting radiative cooling term is

$$\varepsilon\sigma\left(T_p^4 - T_{sa}^4\right) + \varepsilon\sigma\left(T_p^4 - T_{sg}^4\right) = \varepsilon\sigma\left(2T_p^4 - T_{sa}^4 - T_{sg}^4\right) \tag{6}$$

During steady descent there is also cooling due to tangential flow past both the internal and external parachute surfaces. When the parachute is fully inflated, the tangential cooling may be approximated by considering turbulent flow past a 3-foot flat plate, the length of the individual sails. The internal and external velocity distributions $\left(V_I \text{ and } V_E\right)$ over the parachute have been extrapolated from pressure coefficient data in reference 1 for similar parachute configurations. Appropriate values of the internal and external velocities are substituted

into equation (2) to determine an internal heat transfer coefficient $\left(h_{t_{int.}}\right)$ and an external heat transfer coefficient $\left(h_{t_{ext.}}\right)$. The resultant tangential heat transfer coefficient during steady state is $h_t = h_{t_{int.}} + h_{t_{ext.}}$.

Considering normal and tangential convective terms and the radiative term, the cooling rate C for steady-state descent becomes

$$C = \left(h_t + h_n\right)\left(T_p - T_a\right) + 2\varepsilon\sigma\, T_p^{\,4} - (\varepsilon\sigma)\left(T_{sa}^{\,4} + T_{sg}^{\,4}\right) \qquad (7)$$

The coefficients h_t and h_n are of the same order of magnitude — approximately 2 or 3×10^{-3} $Btu/ft^2/sec^2$ for the sail material.

The equations for the cooling term C apply to the parachute sail material and the tape. However, the tape is approximately five times more dense, hence there is negligible cooling due to flow through the material and $h_n = 0$.

Opening Stage $\left(t_c = 10 \text{ sec to } t_c = 12.5 \text{ sec}\right)$

During the opening process, the flow patterns and hence the heat transfer processes are very difficult to analyze. Therefore, further approximations have been made for the transition from reefed conditions to those of steady-state descent. The change of four quantities must be approximated in order to calculate the cooling rate. They are internal and external velocities parallel to the parachute surface, effective length in the flat plate equation, and h_n, the heat transfer coefficient due to flow through the sail material. The external velocity is assumed to be the descent velocity. The other quantities are assumed to vary linearly with time from their values at disreefing to their values during steady-state descent.

The radiative cooling during opening is the same as that for steady descent. The expression for C remains the same as that for steady state (eq. (7)); however, the expressions for h_n and h_t are modified as stated. Here again $h_n = 0$ when calculating tape temperature.

While the above discussion has emphasized the Apollo parachute configuration and deployment sequence, the general approach for determining the cooling rate should apply to other similar situations.

METHOD OF ANALYSIS — DROGUE PARACHUTES

The previous analysis may be applied to ringslot or ringsail parachutes constructed of a porous fabric. However, the Apollo drogue parachutes are fist-type parachutes and must be analyzed in a different manner.

The Apollo drogue parachutes are illustrated in figures 5 and 6 in the reefed and fully inflated configurations, respectively. Each gore of the parachute is constructed of interlaced nonporous ribbons of nylon tape in a square lattice arrangement. The detail of individual gore construction is illustrated in figure 7. The drogue parachute is made of 16 such gores. Air flows through the rectangular slots in the lattice pattern of the ribbons.

Heat transfer to this type of parachute was experimentally investigated during the research reported in reference 2. The correlations developed therein are used in the current study to predict heat transfer to the Apollo drogue parachutes. Schoeck, Hood, and Eckert (ref. 2) found that the heat transfer coefficients for the ribbons of fist-type parachutes could be represented by an equation of the form

$$N_{u_{av}} = K\left(R_e\right)^m = \frac{hl}{k} \tag{8}$$

where K and m are experimentally determined constants. The characteristic length in both the Nusselt number and the Reynolds number is the ribbon width. The velocity used in the Reynolds number is the average velocity between ribbons using incompressible continuity relations and assuming no contraction of the flow. Upstream and downstream Nusselt numbers are determined in reference 2 so that the cooling term C associated with the drogue parachutes becomes

$$C = \left(h_{up} + h_{down}\right)\left(T_d - T_a\right) - 2\varepsilon\sigma T_d^{\,4} + \varepsilon\sigma\left(T_{sa}^{\,4} + T_{sg}^{\,4}\right) \tag{9}$$

The temperature history is then computed numerically from equation (1).

In applying the above method to the Apollo drogue parachutes, the drogue temperature was calculated for the least dense ribbon, the vertical 70-lb nylon tape with a width of 5/8 inch (see fig. 7). For the Reynolds number of range of interest, approximately 10^5, the Nusselt number relations are

$$N_{u_{up}} = 0.46\left(R_e\right)^{0.50} \text{ and } N_{u_{down}} = 0.10\left(R_e\right)^{0.66} \tag{10}$$

The only trajectory variable influencing the heat transfer is the descent velocity. The average velocity between ribbons depends upon the parachute configuration (reefed or disreefed) and the descent velocity. To calculate this average velocity, it is assumed that the volume of air swept out by the parachute flows incompressibly through the slots between the ribbons so that

$$V_{slot} = V_\infty\left(\frac{A_c}{A_s}\right) \tag{11}$$

where A_c is the area of the drogue chute opening and A_s is the slot area.

The Apollo drogue parachute is deployed 16 seconds after abort initiation and is disreefed at 24 seconds. Obviously, the area swept out by the parachute increases from the reefed to the disreefed configuration; therefore, the average velocity and the cooling rate increase after disreefing. The area of openings between the ribbons is 42.8 ft^2. The area swept out by the reefed parachute is 25.1 ft^2, while the area swept out by the disreefed parachute is 72.5 ft^2. The result is that reefed $V_{slot} = 0.586\ V_\infty$ and fully open $V_{slot} = 1.7\ V_\infty$, which results in a substantial cooling rate increase after disreefing. The free stream velocity V_∞ is decreased somewhat after disreefing; however, the net effect is still increased cooling rate.

FIREBALL ESTIMATE

The heating term Q in equation (1) must be estimated for the particular booster involved. Heating rates generated by a Saturn V booster have been estimated semiempirically from observations of other booster explosions (ref. 3). Figure 8, which was developed in reference 3, illustrates the peak heating rate as a function of distance for three different fireball surface temperatures. A surface temperature of 2500° F was used in the present study. An estimate of the time dependence of the peak heating at any location is given in figure 9 and is based on extrapolation of similar data for the explosion of smaller boosters. It should be emphasized that this is a very approximate representation of the booster heat pulse.

After completion of the present analysis, a more rigorous study of Saturn V fireball characteristics was presented in references 4 and 5. The local heating rates of figure 8 are somewhat higher and the pulse duration of figure 9 is longer than similar predictions in the above referenced studies. Therefore, the estimates of heat load to the parachutes generated by an exploding Saturn V used in this report are somewhat higher than would be predicted by the analysis of references 4 and 5.

APPLICATION OF THE ANALYSIS TO AN APOLLO ABORT

The results of the foregoing analysis have been programed for digital computer solution. To illustrate the utility of the analysis in studying a problem of practical interest, the techniques were applied to the determination of temperature histories for several Apollo abort situations. The boundary-condition temperatures used for this analysis are: ambient air temperature T_a = 100° F; radiation source temperature to the atmosphere T_{sa} = 0° R; and radiation source temperature of the ground T_{sg} = 100° F. While it is difficult to obtain general conclusions about the heating and cooling of parachutes from examining results for a specific problem, it is instructive to observe the parachute temperature histories and interpret certain trends in the data in terms of the physical parameters involved.

Trajectory Parameters

Prior to discussing the actual results for Apollo abort situations, the parameters determining and describing the various abort trajectories will be discussed.

Several factors influence the trajectory of the command module during an abort situation and certain combinations of these factors define limiting trajectories which are pertinent to this study. The factors are wind magnitude and direction, initial pitch and pitch rate of the launch vehicle, location of the command module center of gravity, and the alinement of the thrust of the launch escape system rockets. Nominal conditions would correspond to no wind, no initial pitch or pitch rate of the launch vehicle, and no deviation from nominal values for the location of the command module center of gravity and the alinement of the escape rockets. The term "uprange" is used to refer to unfavorable conditions or values of any of the above parameters which would result in an abort trajectory with a landing point closer to the pad than the landing point for a nominal trajectory. "Downrange" refers to trajectories with landing points further from the pad than nominal.

The following trajectories were analyzed in the present study:

1. All conditions nominal except winds which were maximum allowable with a velocity of 37.5 fps opposing the flight of the vehicle.

2. All conditions nominal except winds as in 1 above and maximum allowable unfavorable launch escape vehicle thrust misalinement.

3. Initial pitch of -5° and an initial pitch rate of -1° per second, with maximum unfavorable winds. These initial values are the Apollo emergency destruct system limits; however, the conditions do not correspond to a currently defined Saturn V failure on the pad. However, the above initial conditions are possible for a Saturn IB pad abort. Because all possible failure modes for the Saturn V were not finalized at the time of this calculation, this case is included to illustrate potential problems for off-nominal trajectories.

4. Abort from a nominal Saturn booster in flight at an altitude of 791 feet, with maximum unfavorable winds and maximum allowable launch escape vehicle thrust misalinement. At higher abort altitudes, the launch escape vehicle would always be further away from a nominal booster, therefore less affected by potential booster explosion.

For presentation of results, trajectories will be identified as 1, 2, 3, or 4, corresponding to the above conditions.

Results and Discussion

The results of calculations for representative Apollo abort trajectories are presented in figures 10 to 23.

Figure 10 illustrates the trajectory for an abort from a static booster by a nominal Apollo launch escape vehicle (trajectory 1). Figure 11 is a typical parachute temperature history for this trajectory. It is of interest to interpret certain trends in the data in light of the physical parameters involved. Since the explosion time is at $t_c = 5$ sec, both the tape and the sail material cool from their assumed initial temperatures of 100° F to approximately ambient temperature. When heating begins at $t_c = 5$ sec, the temperatures begin to rise with the tape lagging because of its greater thickness. At $t_c = 10$ sec the opening process begins and the sail material experiences the additional cooling effect due to flow through the nylon. The tape temperature continues to rise at 12.5 seconds while the parachute is in steady descent and the heat pulse from the booster is constant. The slight increase in sail material temperature is due to wind drift in the direction of the launch pad. The slight decrease in temperature just before landing occurs because the heat pulse is beginning to decay from its peak value. The tape, without the benefit of cooling due to normal flow, continues to increase in temperature. The spacecraft and its parachutes reach the ground at $t_c = 24$ sec. The results, shown in figure 10, indicate that the parachute temperature remains well below the maximum allowable temperatures for the Apollo main parachutes of 300° F for a two-parachute descent, and 400° F for a three-parachute descent established in reference 6.

Figure 12 illustrates the effect of explosion time on the maximum temperature experienced by the parachute. The calculation indicates that for the nominal abort trajectory (fig. 10) there are no explosion times which result in tape temperatures above 296° F and sail temperatures above 178° F, both below the maximum allowable temperature. Since time is measured from parachute deployment, negative times indicate explosions prior to deployment. It should be emphasized that this curve is not a temperature history but a representation of the maximum temperature associated with the temperature history for a given time of explosion.

Figure 13 is a drogue temperature history for the nominal abort trajectory with a booster explosion 15 seconds after abort (12.7 seconds before main parachute deployment). The parachute begins to cool at deployment, but the temperature increases toward a maximum of 104° F as the heat pulse increases. At disreefing there is a substantial increase in the cooling and an accompanying decrease in temperature due to the higher velocity between the ribbons as previously discussed.

Figures 14 and 15 are the trajectory and temperature history, respectively, for a pad abort from a static booster with maximum allowable unfavorable thrust alinement of the launch escape rockets (trajectory 2).

The booster was assumed to explode at parachute deployment $\left(t_c = 0\right)$. This particular explosion time resulted in the maximum parachute temperatures for the trajectory. The tape reached 318° F while the sail reached 210° F. Figure 15 indicates trends similar to those noted in figure 11. The decline in the temperatures at 18 seconds is due to the decay in the booster heat pulse. This decline occurred earlier than in trajectory 1 because the booster was assumed to explode 5 seconds earlier.

Figure 16 represents the trajectory for an uprange pad abort with an initial angular rate of -1° per second and an initial pitch of -5° (trajectory 3). This trajectory is included to illustrate the possibility of parachute failure for a postulated off-nominal trajectory. For this trajectory, figure 17 shows that for certain explosion times, namely any time after 7 seconds prior to deployment, the tape temperature exceeds the limit of 400° F. If this trajectory corresponded to a defined failure, a possible solution would be to purposely explode the booster as soon after abort initiation as possible so that the majority of the radiant heat pulse would be spent prior to main parachute deployment. The high temperatures obtained for this trajectory were a direct result of the relatively low range between the parachutes and the booster. The effect on the drogue parachutes of an early booster detonation must be determined. Figure 18 illustrates the drogue temperature history for the slow-divergence uprange abort with a booster explosion 20 seconds after abort initiation. The maximum temperature of drogue chute is shown to be 106° F. This explosion time is sufficiently early (16 seconds before main chute deployment) to prevent main parachute failure.

All the previously discussed cases are based on the assumption that the booster explosion occurred on the launch pad. There is a possibility of an abort condition such that the booster will explode in flight. The computer program developed in this study can account for the explosion of a moving booster if its trajectory is known. Figures 19 and 20 present respectively the trajectory and temperature history for an abort from a moving booster (trajectory 4). The abort was assumed to occur from a nominal Saturn V launch vehicle at an altitude of 791 feet and the launch vehicle was assumed to explode 30 seconds after lift-off. The maximum parachute temperature calculated for this case was 145° F.

As previously stated, it is difficult to generalize the results of these calculations because of the many variables involved. However, there is one conservative generalization that can be made; the analysis can be used to define a distance of closest safe approach such that there will be no failure if during any given trajectory the booster and spacecraft are never closer than this critical distance.

The calculation was performed by fixing the distance from the explosion to the parachute at a constant value. The history of the descent velocity was then specified to correspond to that of a nominal abort. For each fixed distance, the booster explosion time was varied to determine the maximum possible parachute temperature for that distance. These data are presented in figures 21 and 22 for ranges of 2500, 3000, 3500, and 4000 feet. The maximum temperature versus distance for the tape and the sail material can then be plotted (see fig. 23). For a maximum allowable temperature of 400° F, the distance of closest approach is 3850 feet. This means that if during the abort, the parachute were always 3850 feet or more from the booster, the temperature would never exceed 400° F, regardless of the time of explosion. For a maximum allowable temperature of 300° F, the critical distance is 4900 feet.

It should be emphasized that this approach is conservative and should be used only when no trajectory data are available for actual calculation of temperature histories. The degree of conservatism inherent in this approximation may be assessed by considering the results for trajectories 1, 2, and 3.

Trajectory	Minimum range, ft (a)	Maximum sail temp., °F (b)	Sail temp., °F (c)	Maximum tape temp., °F (b)	Tape temp., °F (c)
1	4550	178	210	296	325
2	3800	208	255	318	405
3	2450	435	480	650	---

[a]After deployment.

[b]Based on actual trajectory.

[c]At constant minimum range.

CONCLUSIONS

A method has been developed for applying standard heat transfer techniques to the analysis of the cooling mechanisms associated with parachutes.

The method has been applied to the study of a particular problem, namely the abort of an Apollo spacecraft in the presence of a Saturn V booster explosion. Based on fireball characteristics determined in a

previous study, no Apollo parachute failures from heating from a booster explosion are predicted for nominal abort conditions or for maximum allowable unfavorable thrust alinement of the launch escape vehicle.

If other abort modes are defined in the future for which a parachute failure would be predicted, a possible solution is forced detonation of the booster early enough that the radiant heat pulse will be spent prior to parachute deployment.

A conservative minimum distance of approach is presented which can be used to evaluate abort safety in cases for which trajectory information is not available. Using the assumed characteristics of a Saturn V explosion, this distance for an Apollo abort is 3850 feet for a maximum allowable parachute temperature of 400° F.

The computer program which has been developed is capable of computing temperature histories of the parachutes for any other possible trajectories and can be applied to improved estimates for fireball characteristics as they become available.

APPENDIX

DETERMINATION OF THE EQUIVALENT NORMAL FILM COEFFICIENT FOR AIRFLOW THROUGH THE PARACHUTE

Determination of the convective cooling due to airflow through parachute material requires the determination of a representative normal film heat transfer coefficient corresponding to the conditions of descent after an abort. For the purposes of this analysis, McDonnell Aircraft Corporation's unpublished parachute simulation test data were used in conjunction with a transient heat transfer digital computer program (THTB) to find an effective normal film coefficient. This normal heat transfer coefficient was found to be a function of parachute surface temperature. The analysis used test parameters of initial and final parachute temperatures, heating rates, and time to determine the normal film coefficient which satisfied the test boundary conditions. A computer simulation considered both transient radiation interchange to the test chamber and normal film cooling through the parachute material.

The test results used for the normal flow film coefficient determination were based on unstitched, nonshock-loaded, 1.1-ounce per square yard nylon cloth with normal airflow through the material corresponding to 0.11 inches of H_2O pressure drop across the parachute material. This pressure drop corresponds to that experienced by both the Apollo and Gemini launch escape system parachutes during steady descent. The material tested is the same as the parachute sail material for both spacecraft.

Description of McDonnell Test and Results

Tests were performed at McDonnell Aircraft Corporation to determine if specimens of personnel parachute canopy material would fail when subjected to simulated incident heat flux which would be encountered should a catastrophic booster failure occur during a Gemini launch. The parachute canopy specimens were MIL-C-7020D, type 1, 1.1-ounce per square yard nylon cloth, natural color, and international orange.

The test apparatus consisted of a horizontal radiant heat source and an air supply for simulation of natural airflow through the specimens. The heat source was a cylindrical cavity, the walls of which were inductively heated to approximately 2500° F. The airflow through the material was equal to that experienced by the parachute during a sea level steady-state descent. No tangential airflow was simulated in the test.

The three levels of incident heat flux simulated for the flow conditions were 8.2, 6.85, and 5.6 $Btu/ft^2/sec$. For a given heat flux intensity, the threshold failure point (defined as the first visible evidence of fiber degradation) was determined by varying the exposure time.

The results from the McDonnell tests for the forced airflow cases are shown in figures 24 and 25. Figure 24 presents total incident heat as a function of exposure time required to visibly damage the parachute canopy material. This curve may be used to determine the absorptivity of the nylon parachute material by extrapolating to the zero exposure time intercept. This intercept may be interpreted as the total incident heat required to raise the temperature to 482° F (inception of melting) if there were no cooling losses. This method of determining the total incident heat with no losses is valid since the heat losses from the material by radiation and convection will be a small percentage of the total incident heat for very short exposure times. Based on this approach, it was found that a total incident heat of 7.33 Btu/ft^2 will visibly damage the parachute material if there are no losses. Using reference 7, the specific heat was determined to be 0.55 Btu/lb/°F at the average test temperature of 281° F. This value for specific heat resulted in an absorptivity of 0.23.

Application of Test Results to Determine Normal Film Coefficient

In order to establish the normal film coefficient as a function of parachute temperature, a transient heat transfer digital computer program was used to simulate the McDonnell test conditions. The following conditions were used in the thermal simulation:

a. Initial temperature = 80° F

b. Visible damage temperature = 482° F

c. Air temperature = 100° F

d. Sink temperature = 80° F

e. Material = MIL-C-7020D type 1, 1.1-oz/yd^2 nylon cloth

f. Reradiation interchange from one side of cloth

g. Emissivity of nylon = 0.73

h. Variable specific heat in accordance with reference 4

i. Absorptivity of nylon = 0.23

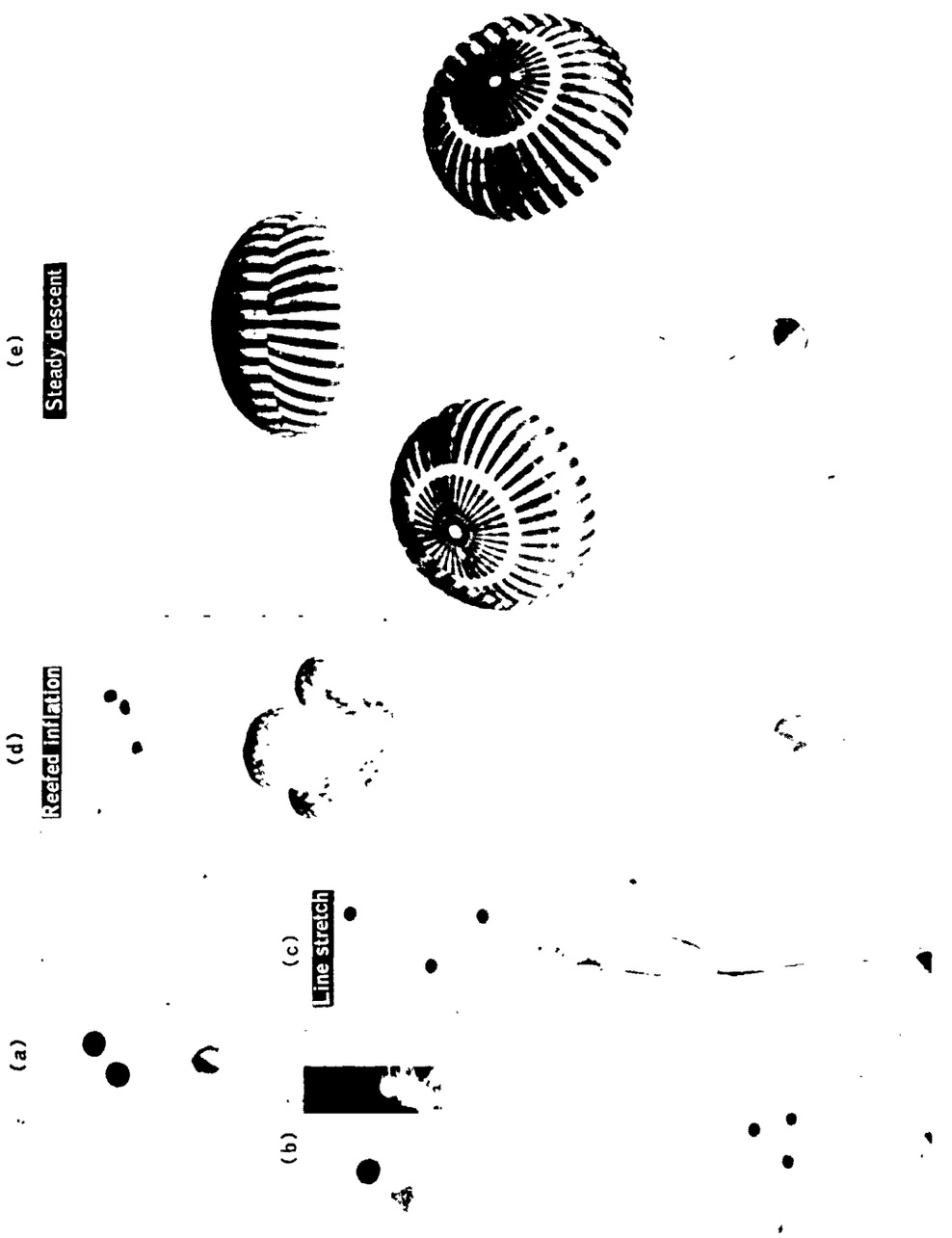

(a) (b) (c) Line stretch (d) Reefed inflation (e) Steady descent

Figure 1.- Parachute opening sequence.

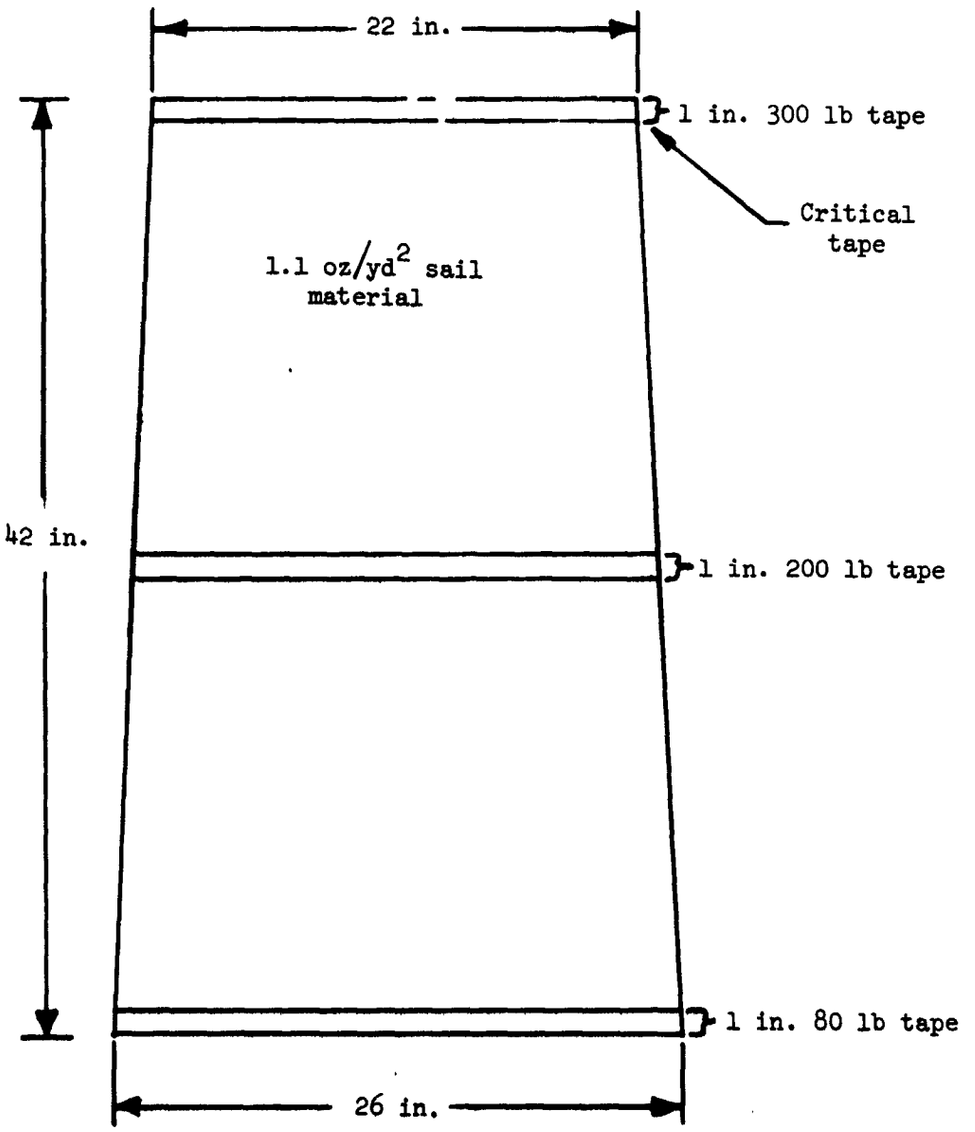

Figure 2.- Detail of critical parachute sail (No. 6)

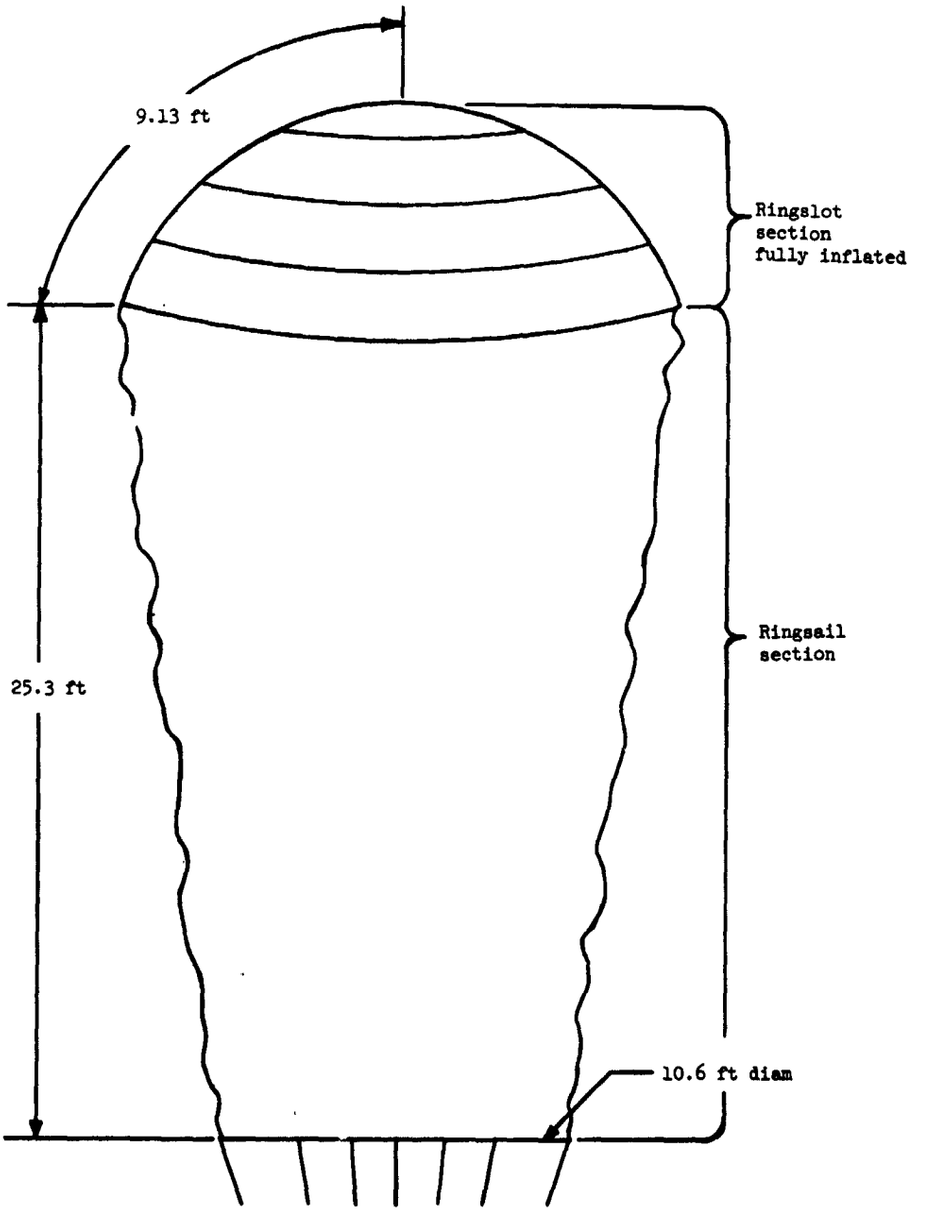

Figure 3.- Schematic illustration — fully reefed inflation.

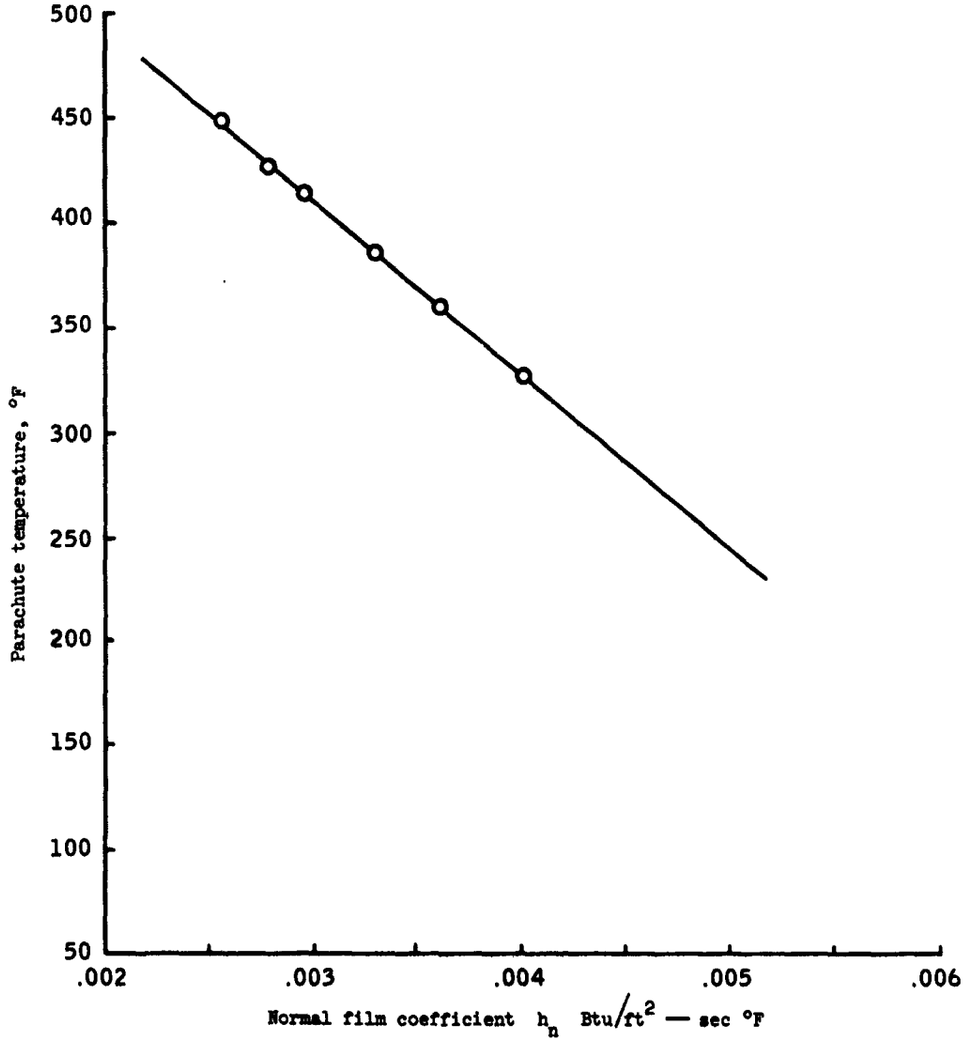

Figure 4.- Normal film coefficient as a function of parachute temperature for 100° F ambient air temperature.

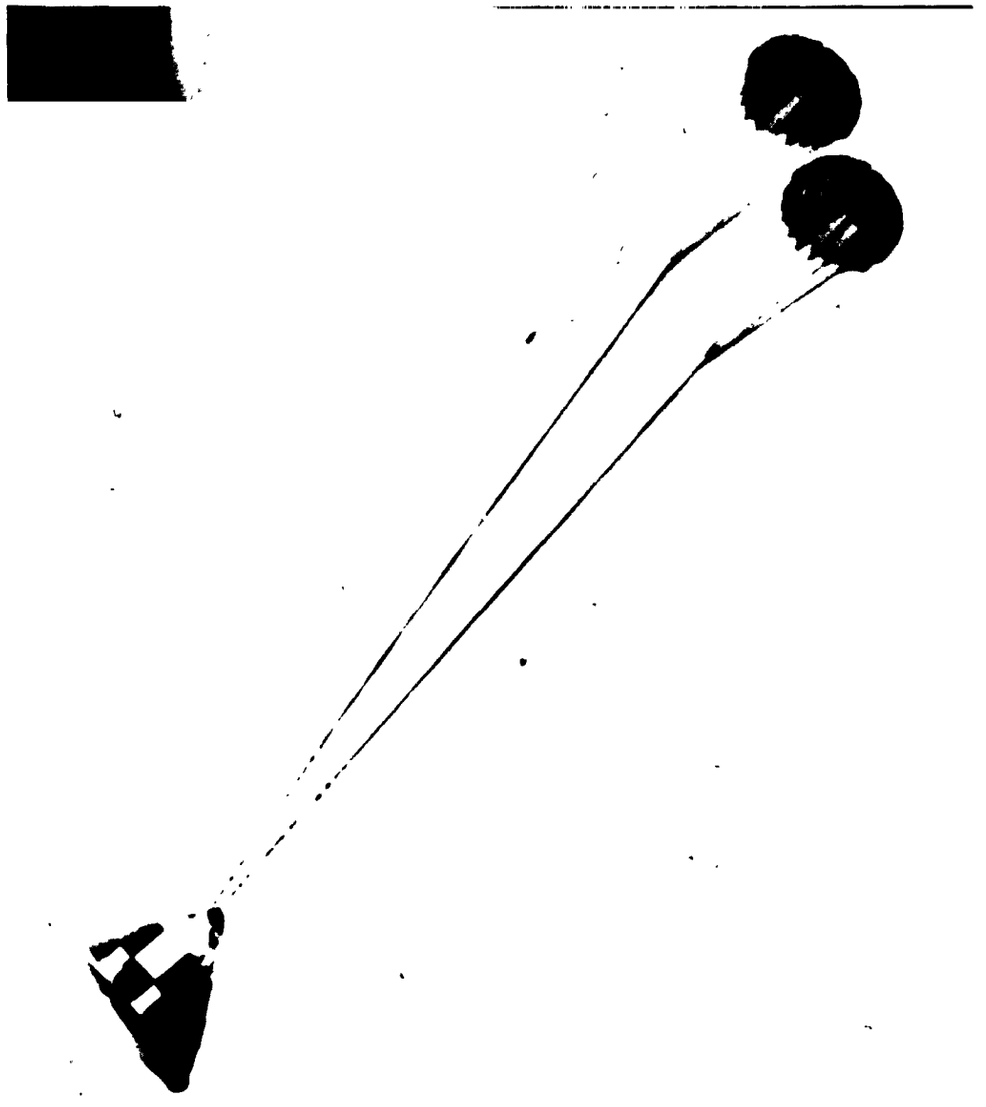

Figure 5.- Drogue parachutes in reefed inflation.

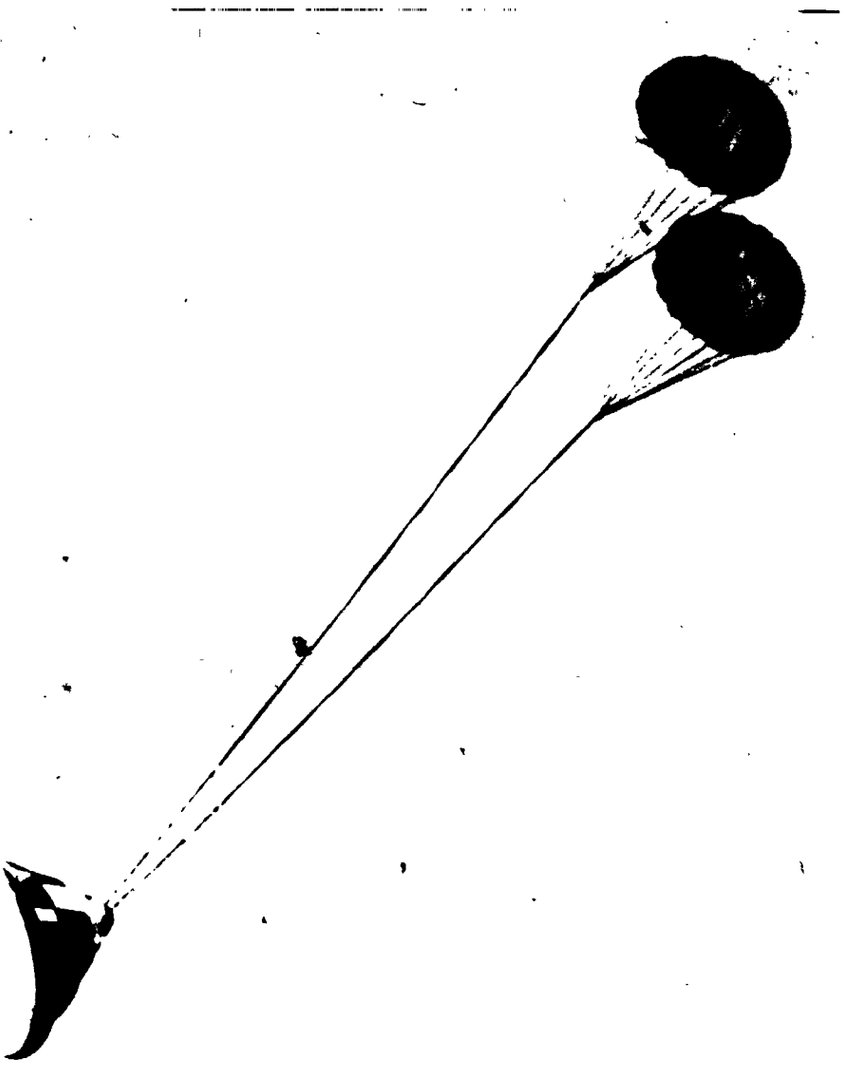

Figure 6.- Fully inflated drogue parachutes.

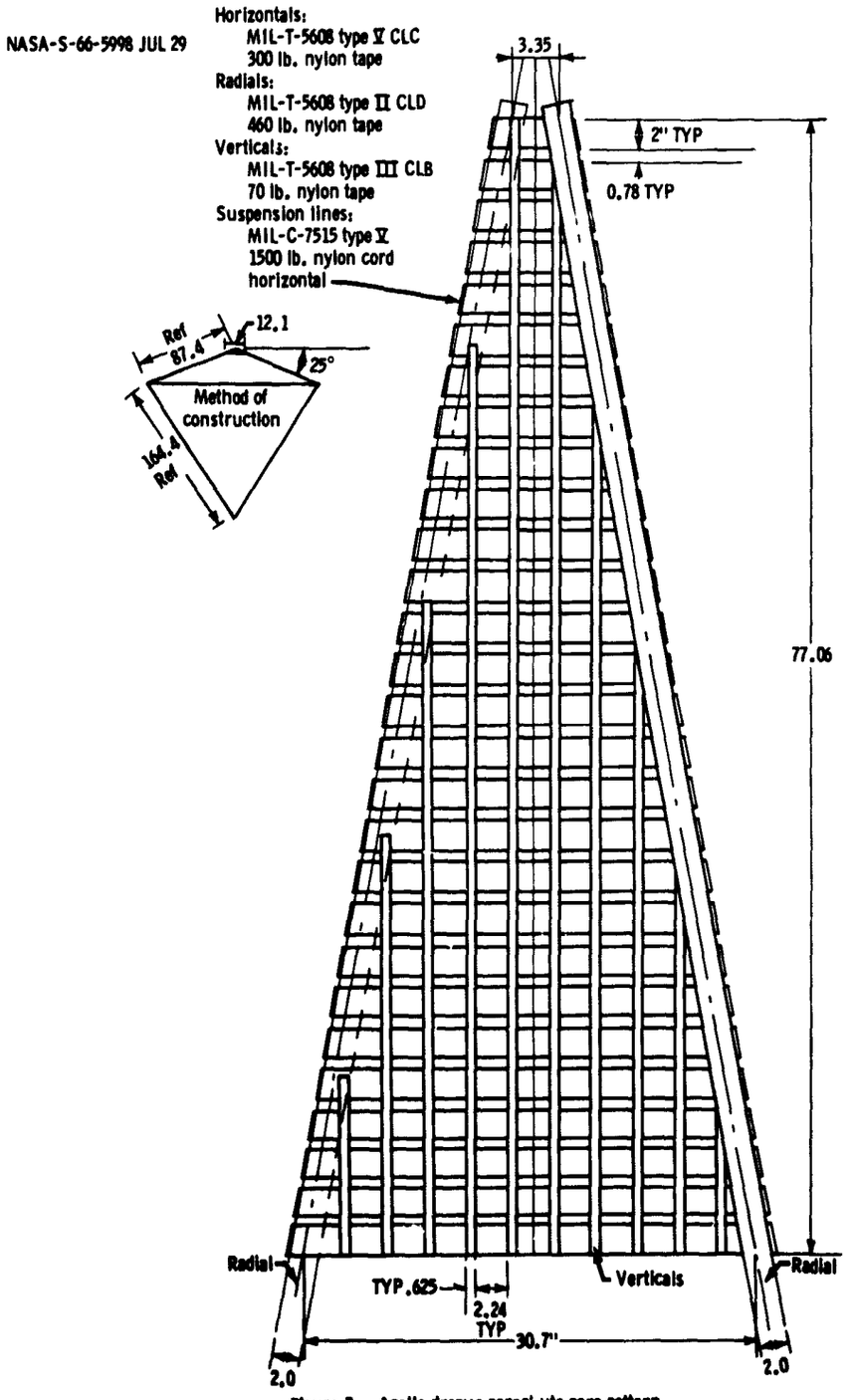

Figure 7. - Apollo drogue parachute gore pattern.

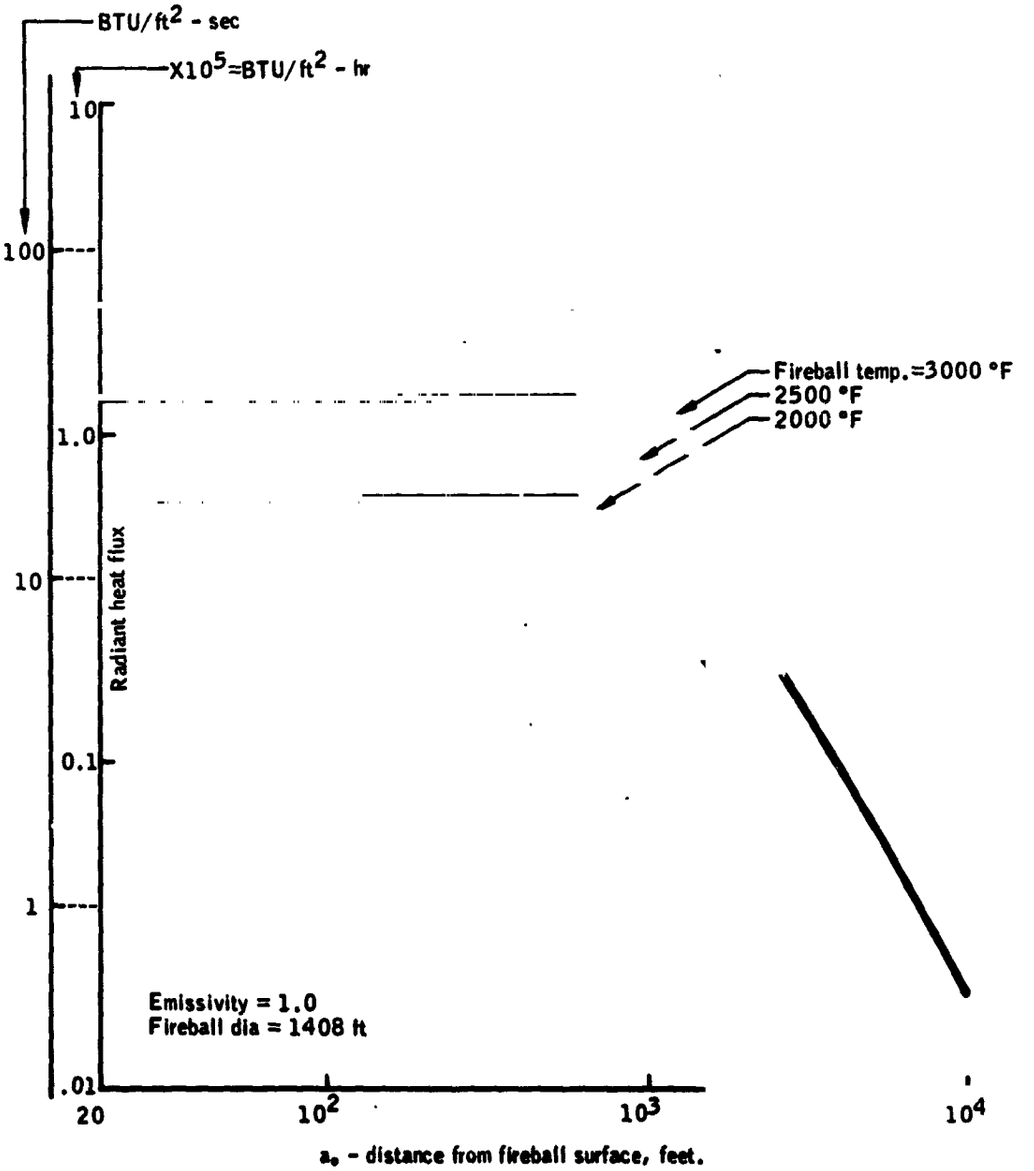

Figure 8.- Saturn V heat flux as a function of distance.

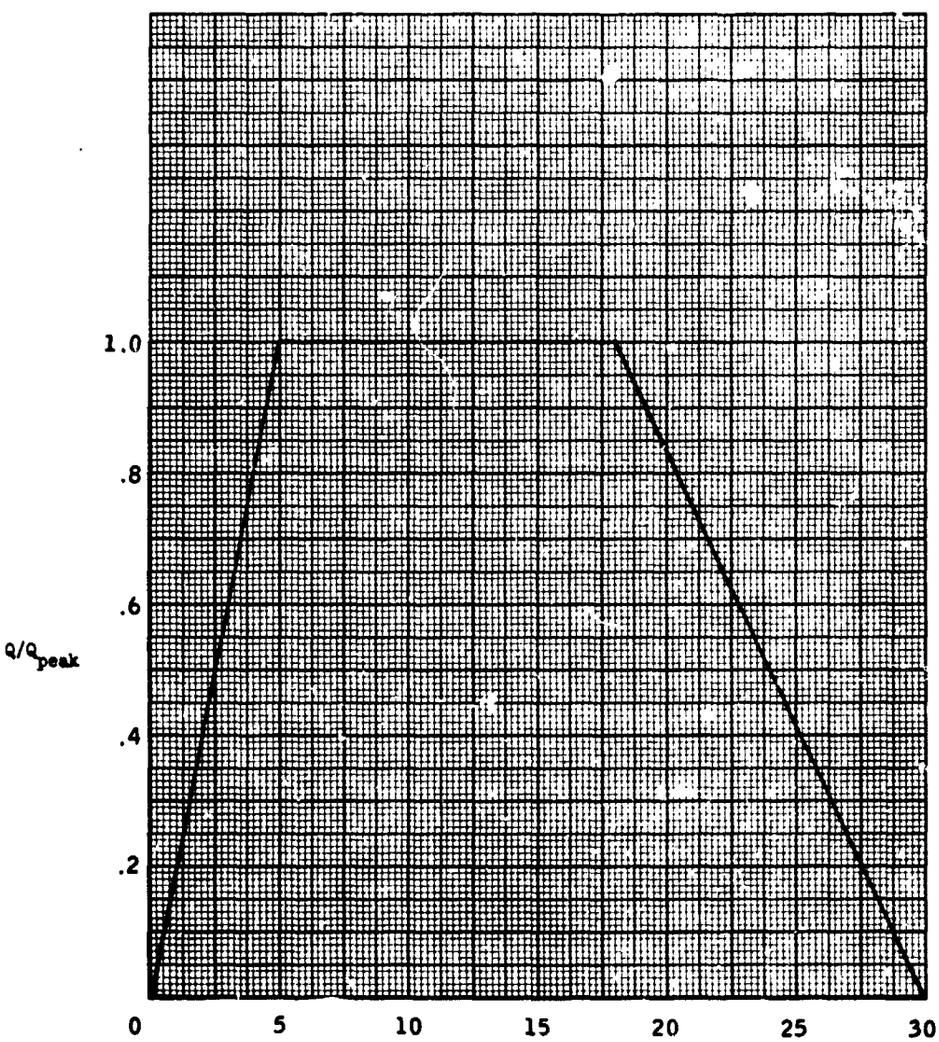

Figure 9.- Saturn V heat flux as a function of time.

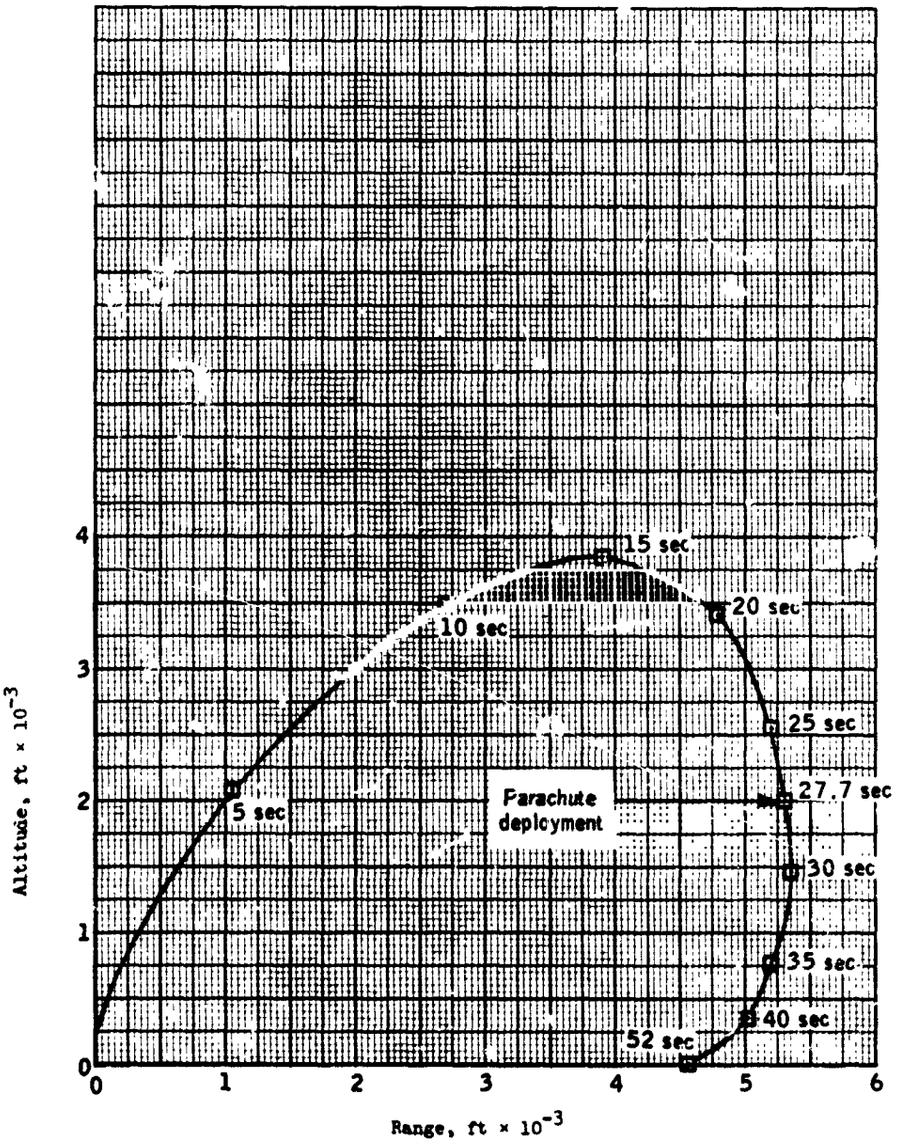

Figure 10.- Nominal pad abort trajectory static booster for maximum unfavorable winds.

Six different incident flux levels from the curves of figures 24 and 25 ranging from a 1-second heat pulse at 12.25 $Btu/ft^2/sec$ to steady-state heating at 4.87 $Btu/ft^2/sec$ were simulated. The average film coefficients required to satisfy these conditions are shown in figure 26. As can be observed from figure 26, the constant values for film coefficients required to satisfy the test results were not the same for each case. Since it appears reasonable to assume that the pressure and coolant air velocity are invariant from case to case for the test conditions, it can be inferred that the temperature dependence of the film coefficient coupled with different time-temperature profiles for each case might explain the variable coefficients.

In attempting to obtain a correlation of normal film coefficient with temperature, a weighted average temperature was determined for each of the simulation cases considered. The average temperature used for each case was obtained by integrating the average temperature over the exposure time as shown in figure 27. The resulting dependence of normal film coefficient on average parachute temperature is shown in figure 28.

Results and Discussion

To determine the validity of the curves of figure 28 relative to the test data, the McDonnell test parameters were simulated on the THTB program using the linear normal film coefficient as a function of parachute temperature. For each time step, the program averaged the parachute temperature at the beginning and end of the time step to determine an average temperature for entry into the film coefficient tables in the program. Comparison of these results are shown below:

Incident flux, $Btu/ft^2/sec$	Response time for melting (482° F), sec	
	Test results	THTB results
12.25	1.1	0.9
8.2	2.2	1.83
5.93	7.0	4.8
5.60	10.9	6.17

In all cases using the variable film coefficient, conservative results were obtained in that the time to reach the parachute melting temperature was less than the test exposure time. The predictions were in better agreement with the test results at the shorter test times since the temperature response at higher flux levels is more linear with time.

The temperatures referred to in figure 27 are parachute skin temperatures rather than an average of the parachute and air temperatures, which are more commonly used when correlating film coefficients. Since the air temperature is assumed constant throughout the tests, no difficulties are introduced by correlating the film coefficient with the average parachute temperature. This factor should be taken into consideration, however, if the film coefficient is used for other than 100° F air temperature. For a more general use of the normal film coefficient, a curve of film coefficient versus average fluid/material temperature is included in figure 28.

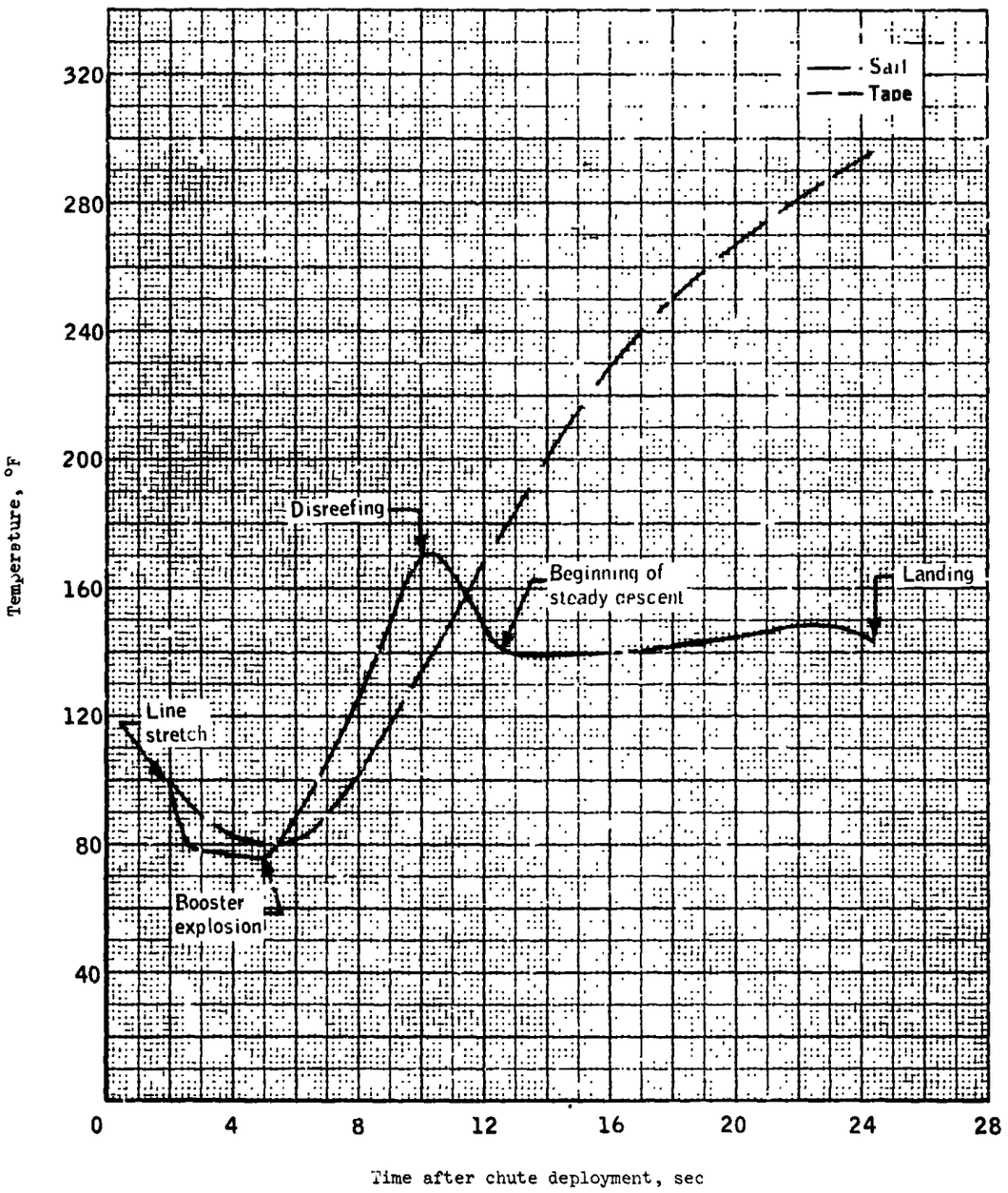

Figure 11.- Parachute temperature history for nominal pad abort, static booster. Booster explosion at t_c = 5 sec.

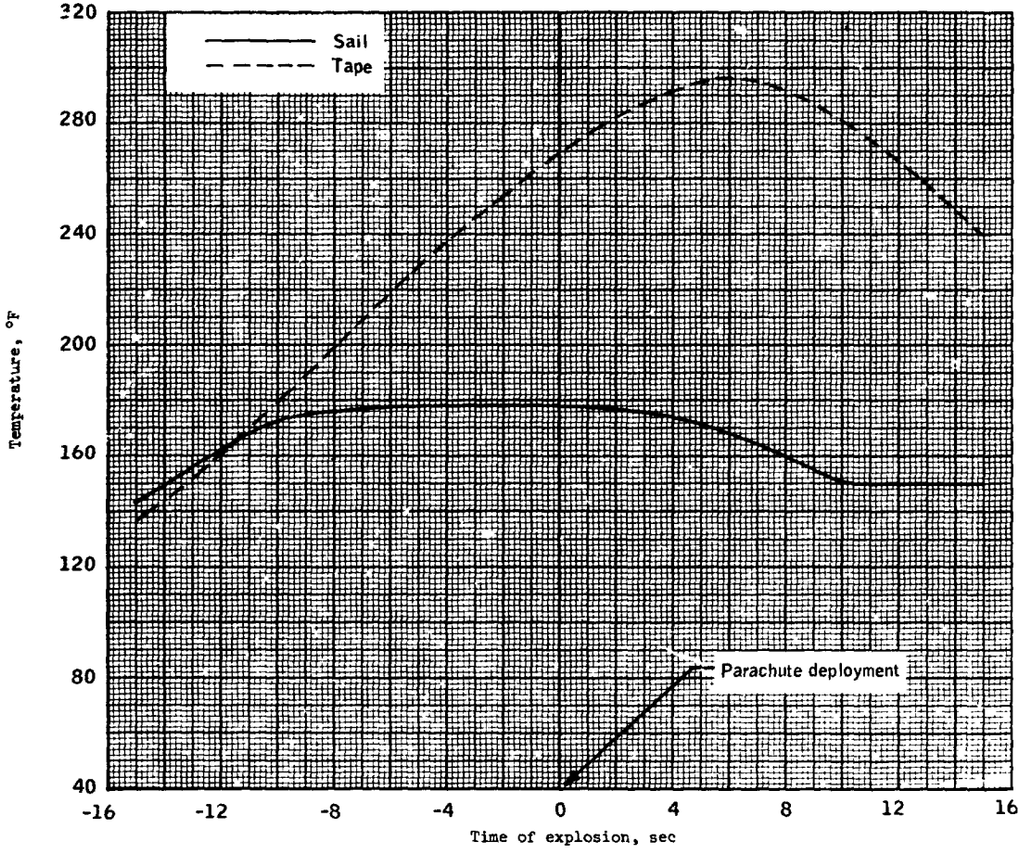

Figure 12.- Maximum temperature as a function of explosion time for a nominal pad abort, static booster.

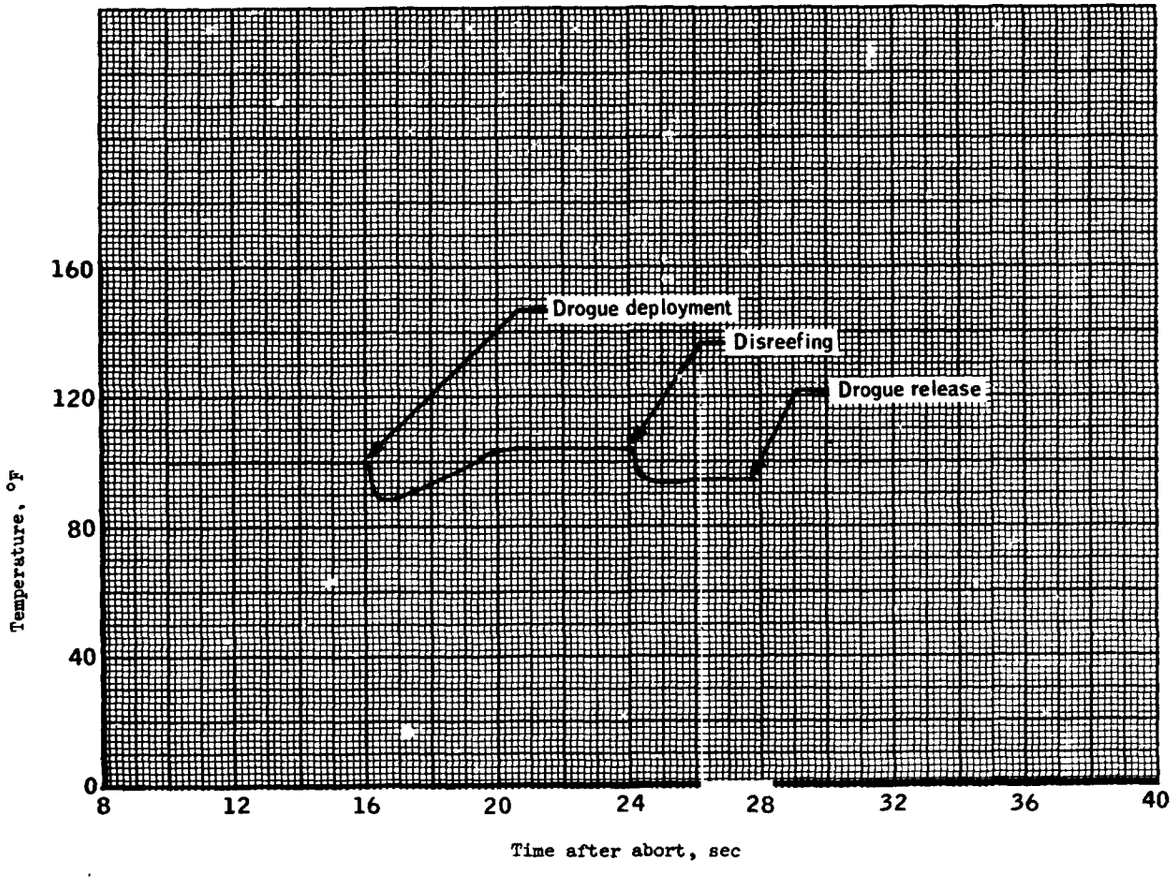

Figure 13.- Drogue temperature history for nominal pad abort, static booster. Booster explosion 15 sec after abort or 12.7 sec before main deployment.

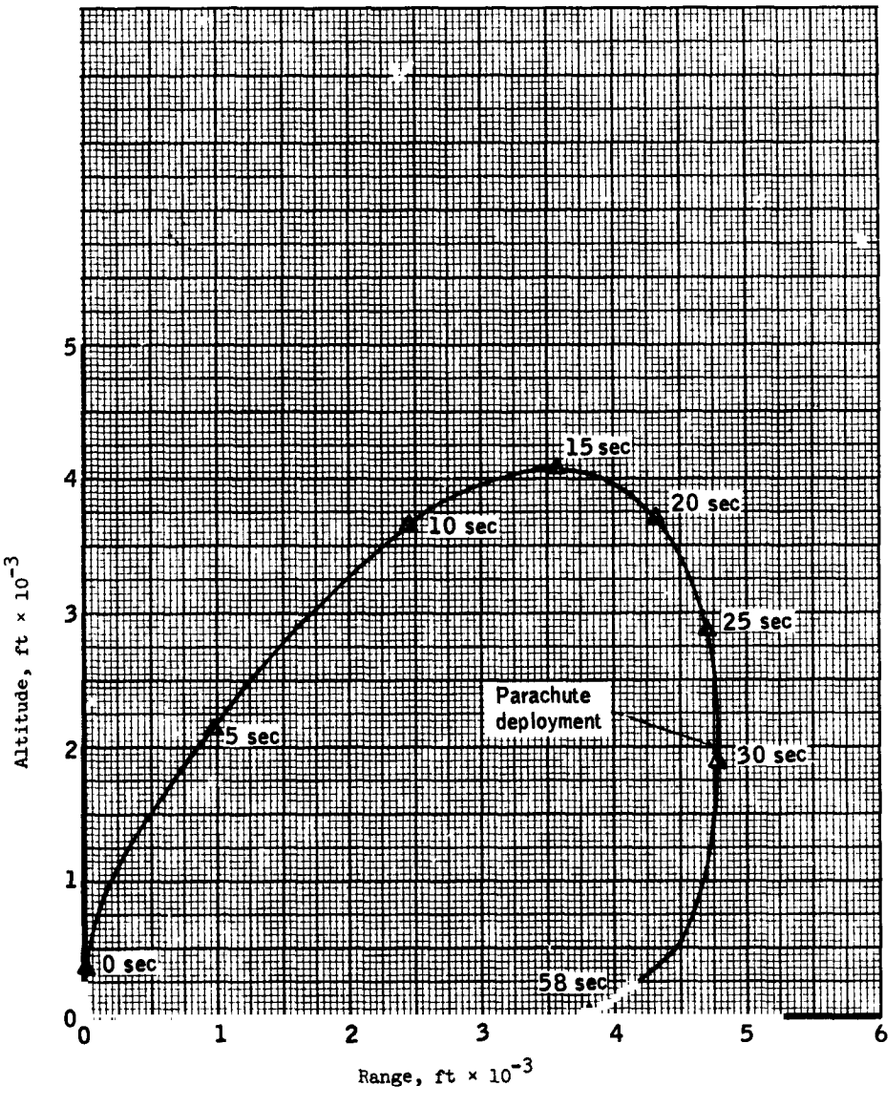

Figure 14.- Pad abort trajectory with maximum allowable LEV thrust misalinement and maximum unfavorable winds.

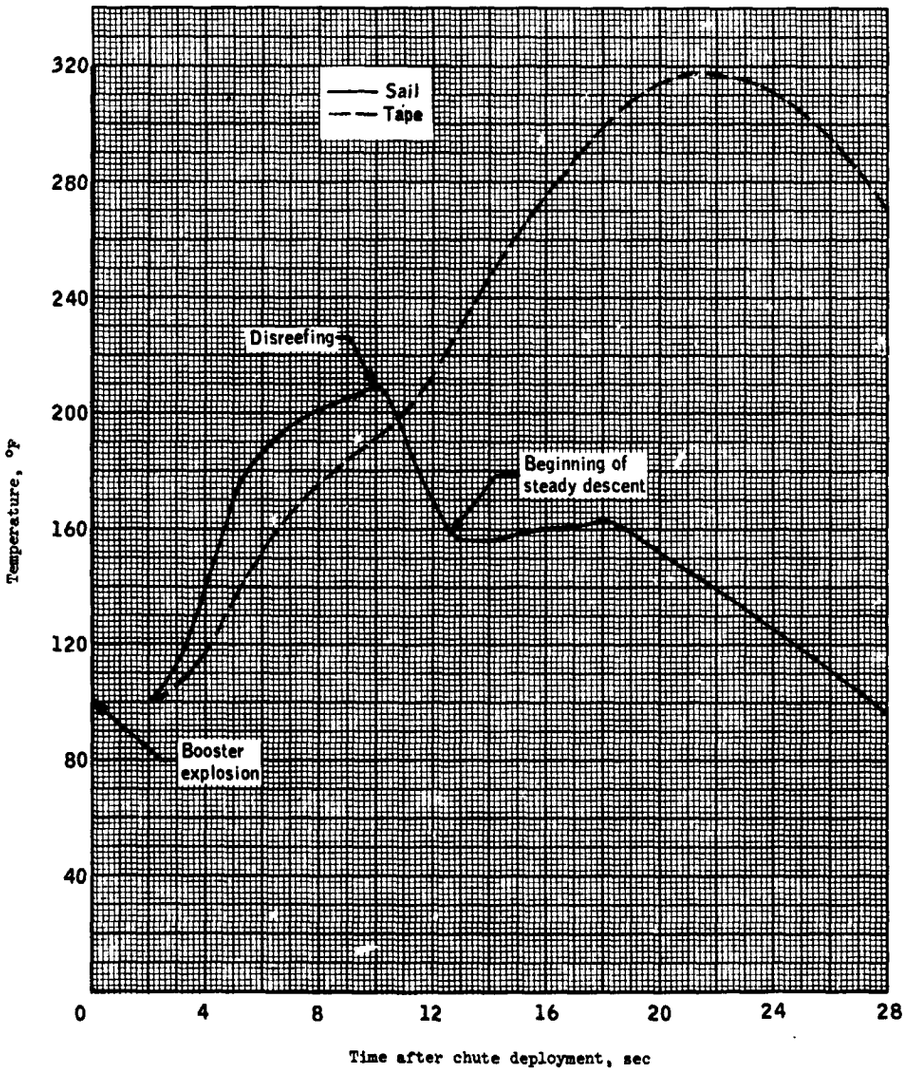

Figure 15.- Parachute temperature history for pad abort with maximum allowable LEV thrust misalinement, booster explosion at parachute deployment.

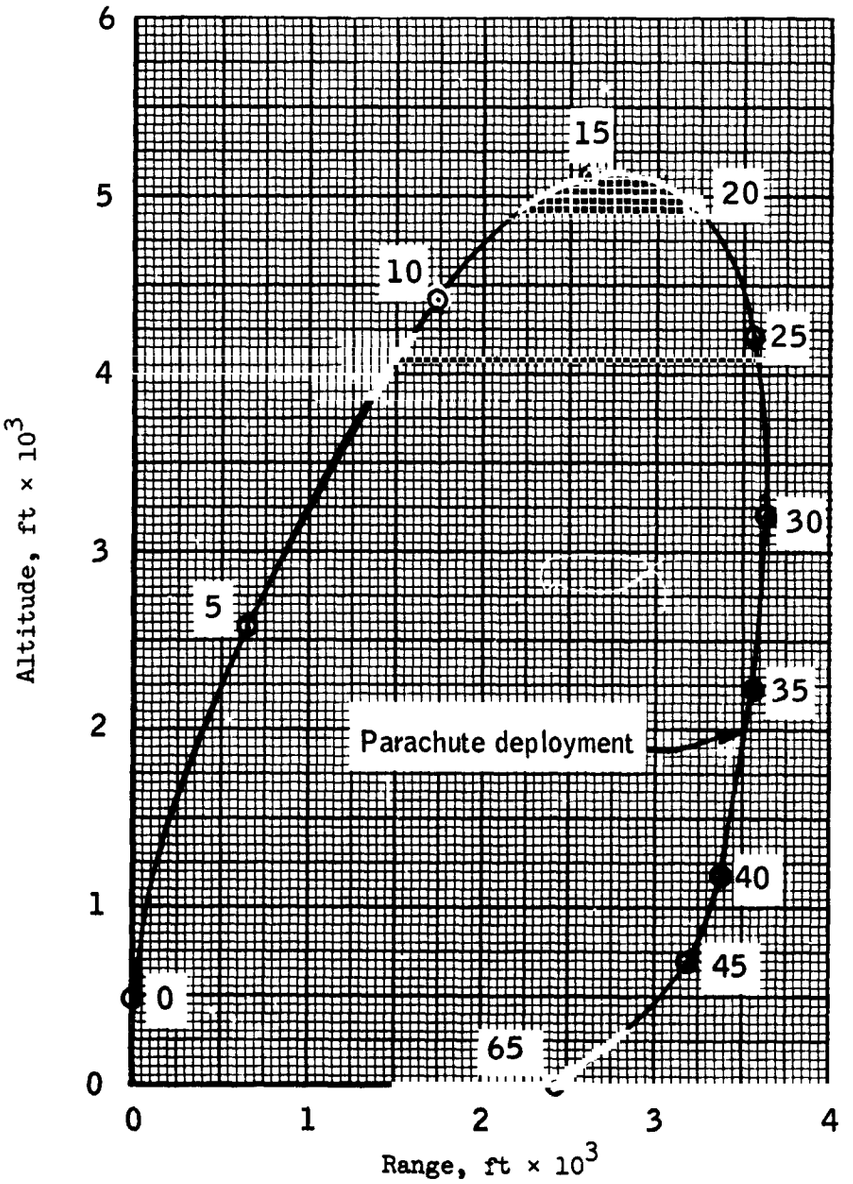

Figure 16.- Trajectory for slow divergence uprange pad abort. Angular rate -1°/sec, pitch -5°.

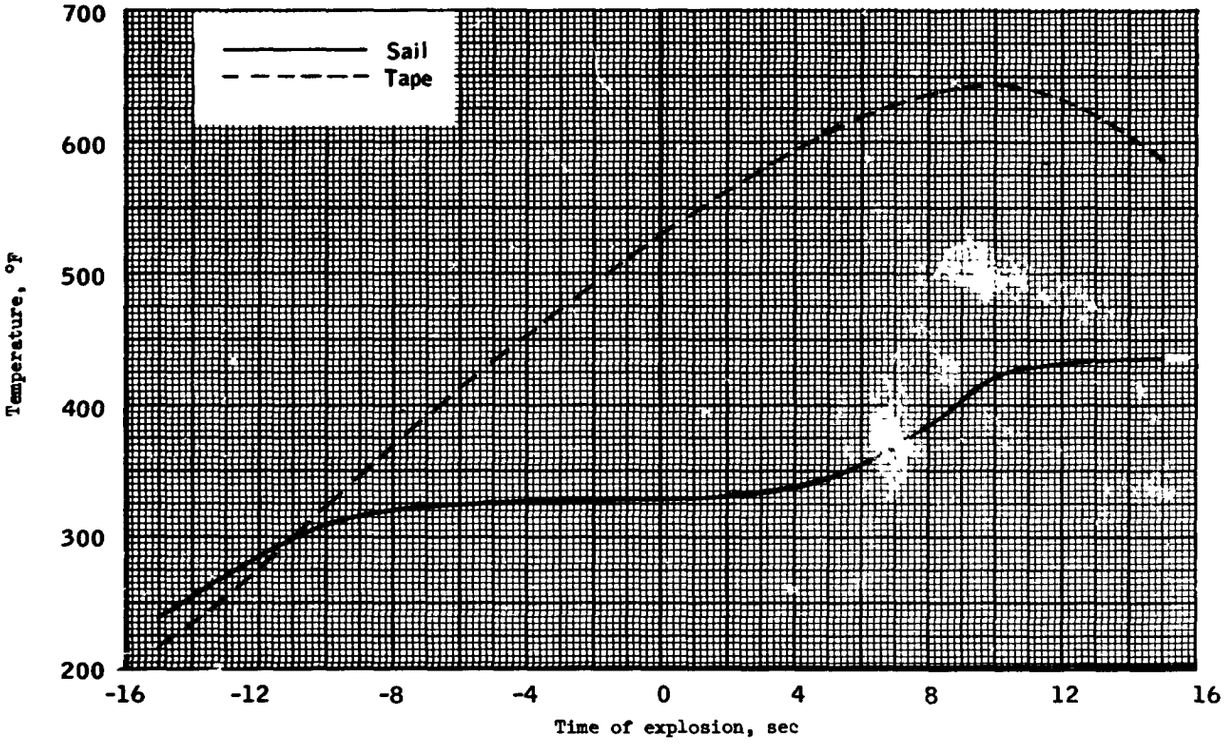

Figure 17.- Maximum temperature as a function of explosion time for slow divergence uprange abort conditions.

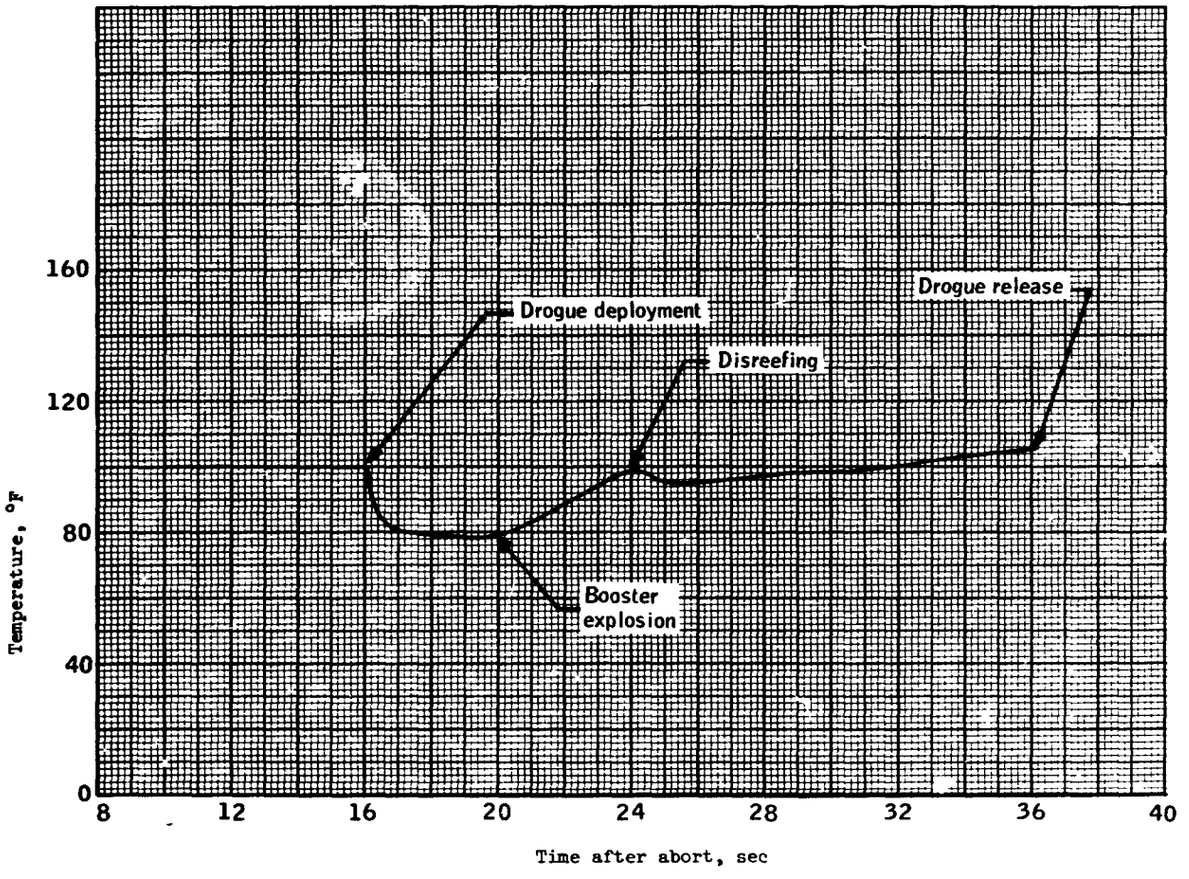

Figure 18.- Drogue temperature history for slow divergence uprange pad abort. Booster explosion 20 sec after abort or 16 sec before main deployment.

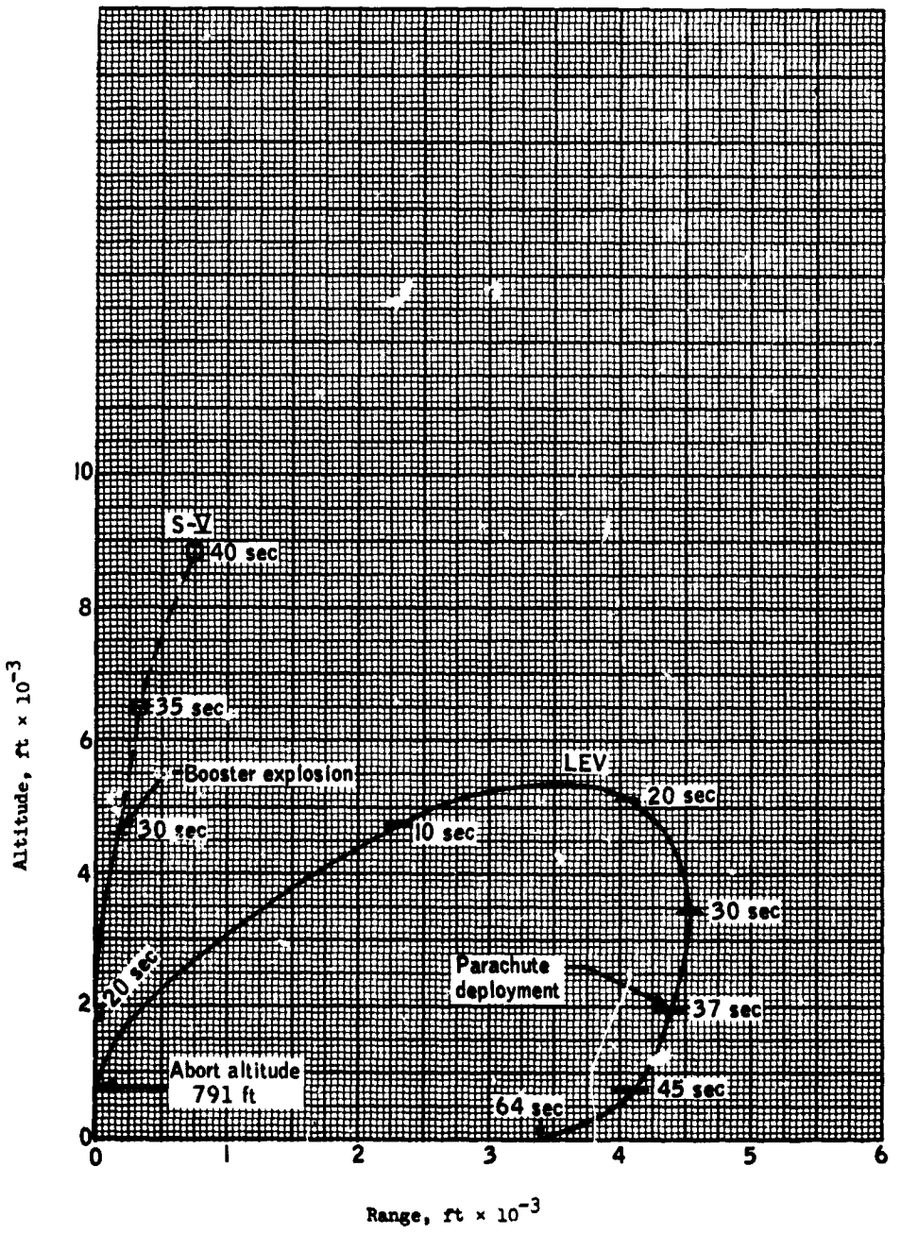

Figure 19.- Abort trajectory from a nominal S-V for maximum allowable unfavorable LEV thrust misalinement.

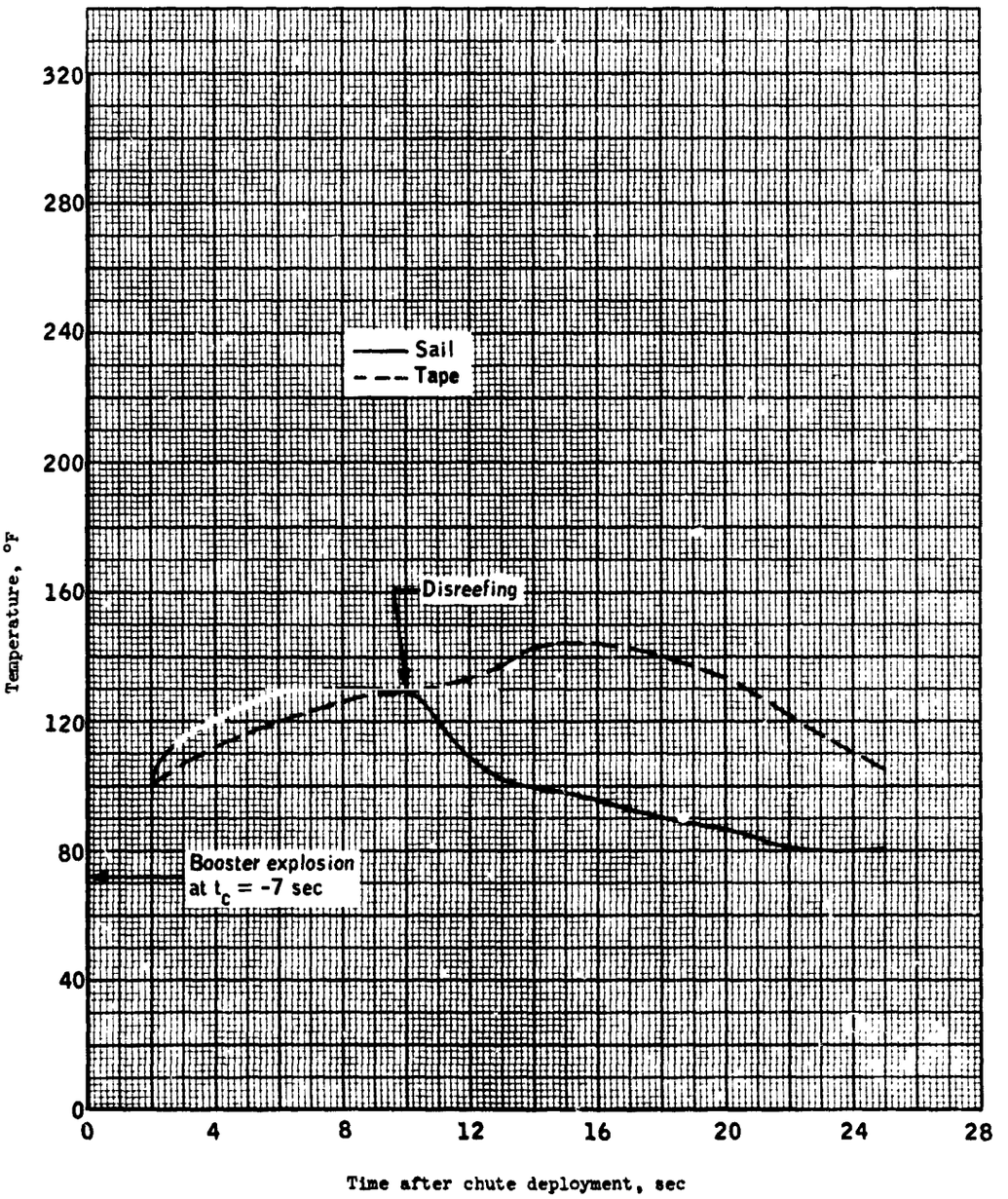

Figure 20.- Parachute temperature history for moving booster. Abort altitude 791 ft and blast time 7 sec before parachute deployment.

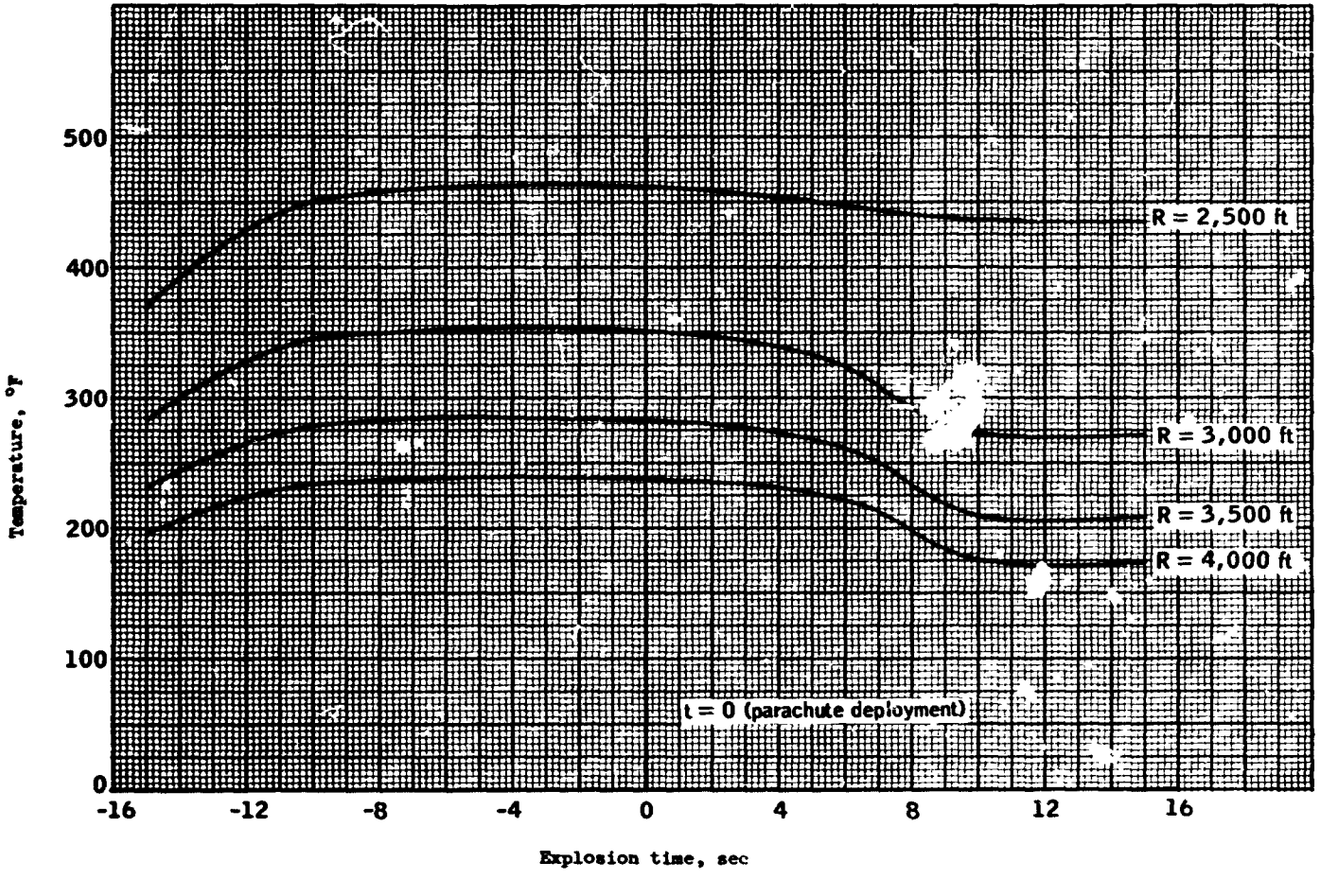

Figure 21.- Sail temperature as a function of explosion time for constant distance from point of explosion.

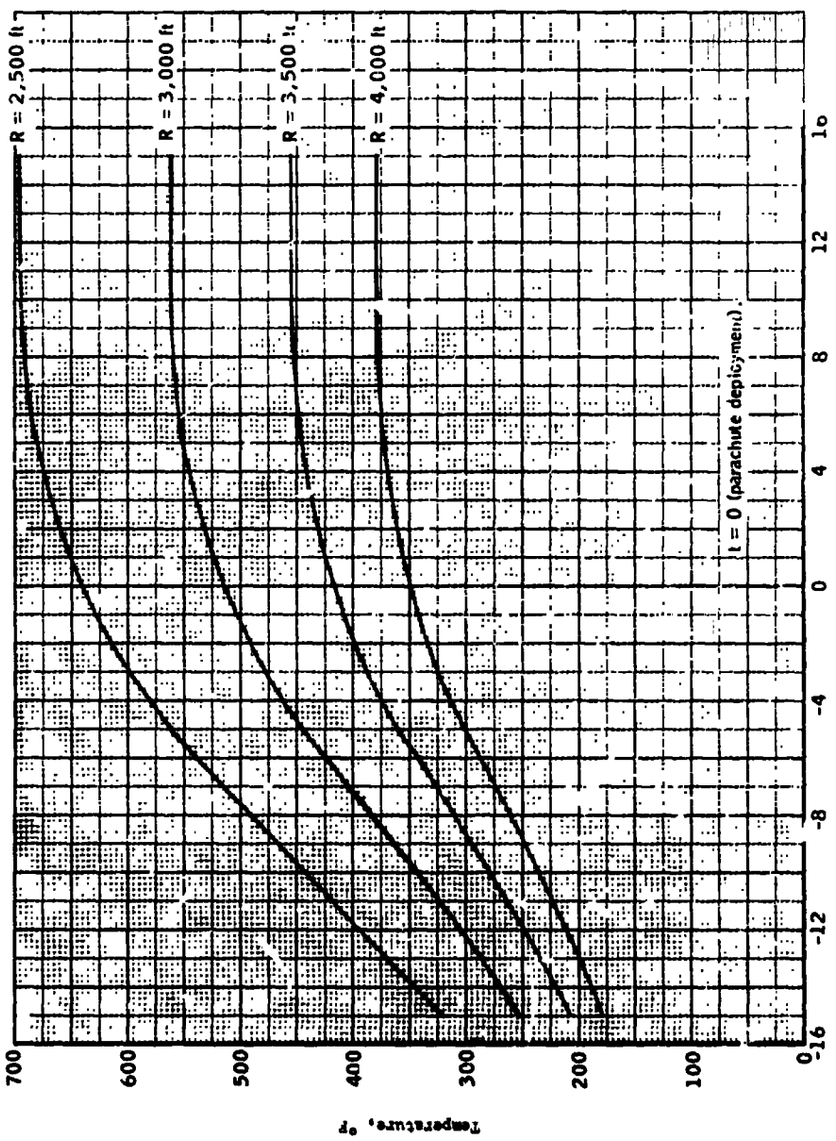

Figure 22.- Tape temperature as a function of explosion time for constant distance from point of explosion.

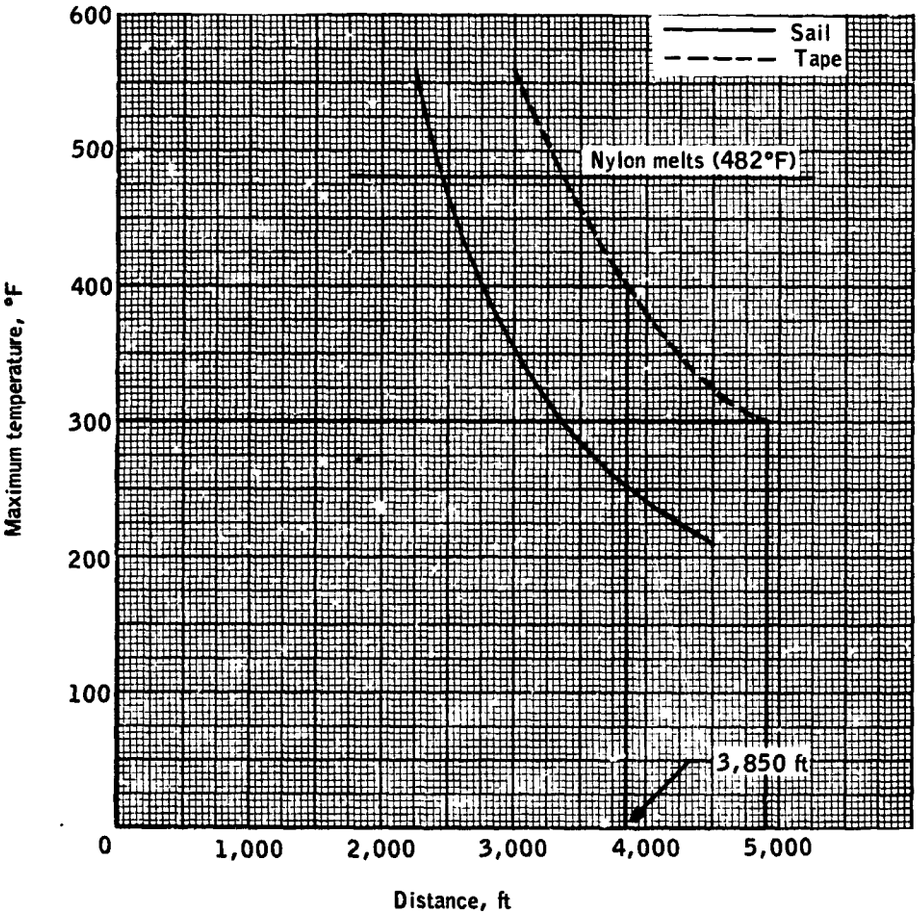

Figure 23.- Minimum range determination.

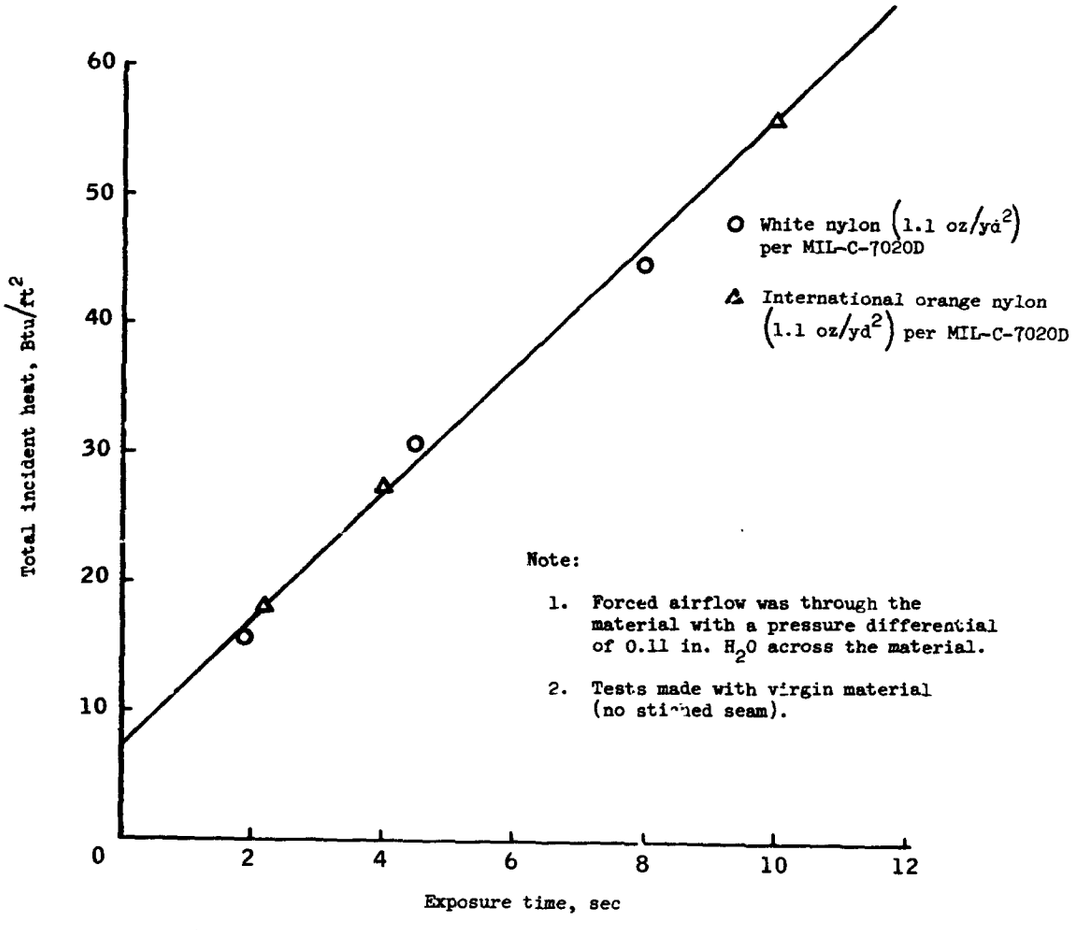

Figure 24.- Heating required to visibly damage material with forced airflow.

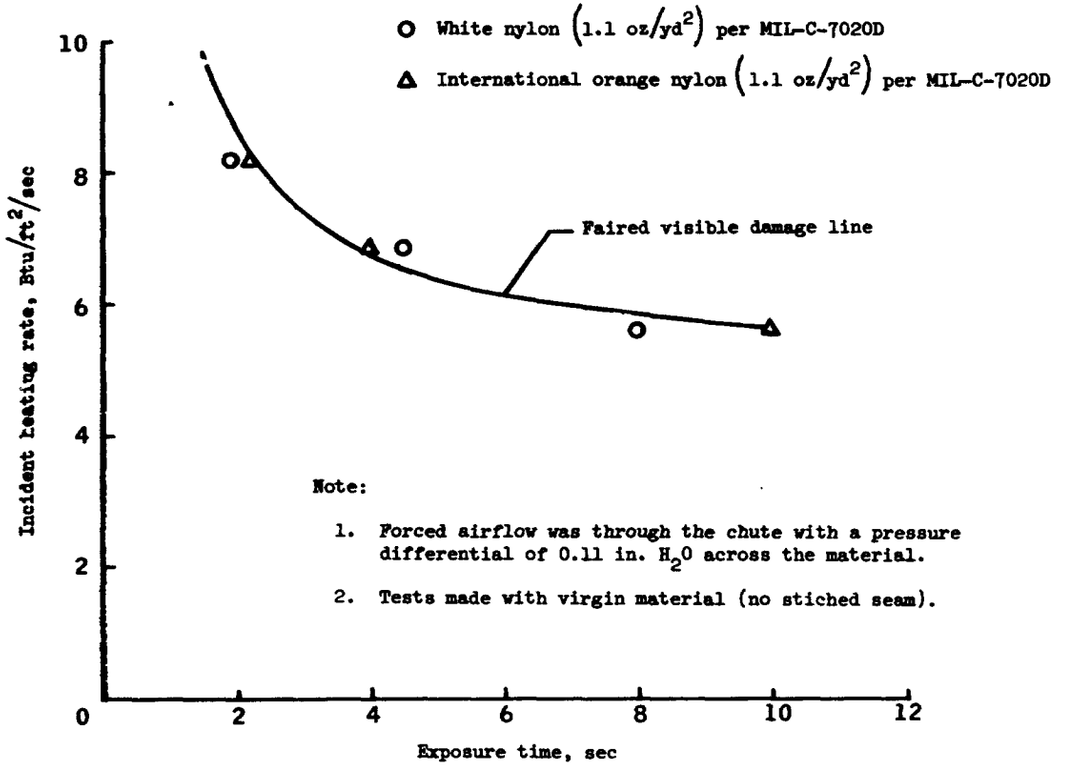

Figure 25.- Heating required to visibly damage material with forced airflow.

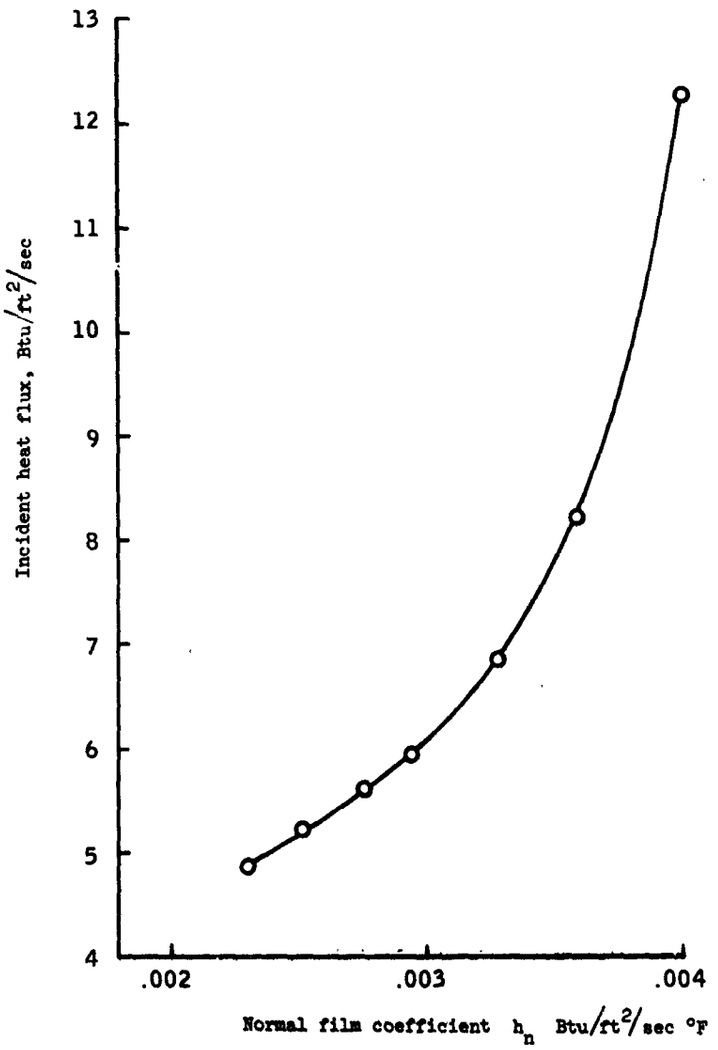

Figure 26.- Normal film coefficient as a function of incident flux calculated with THTB Program with MAC test conditions.

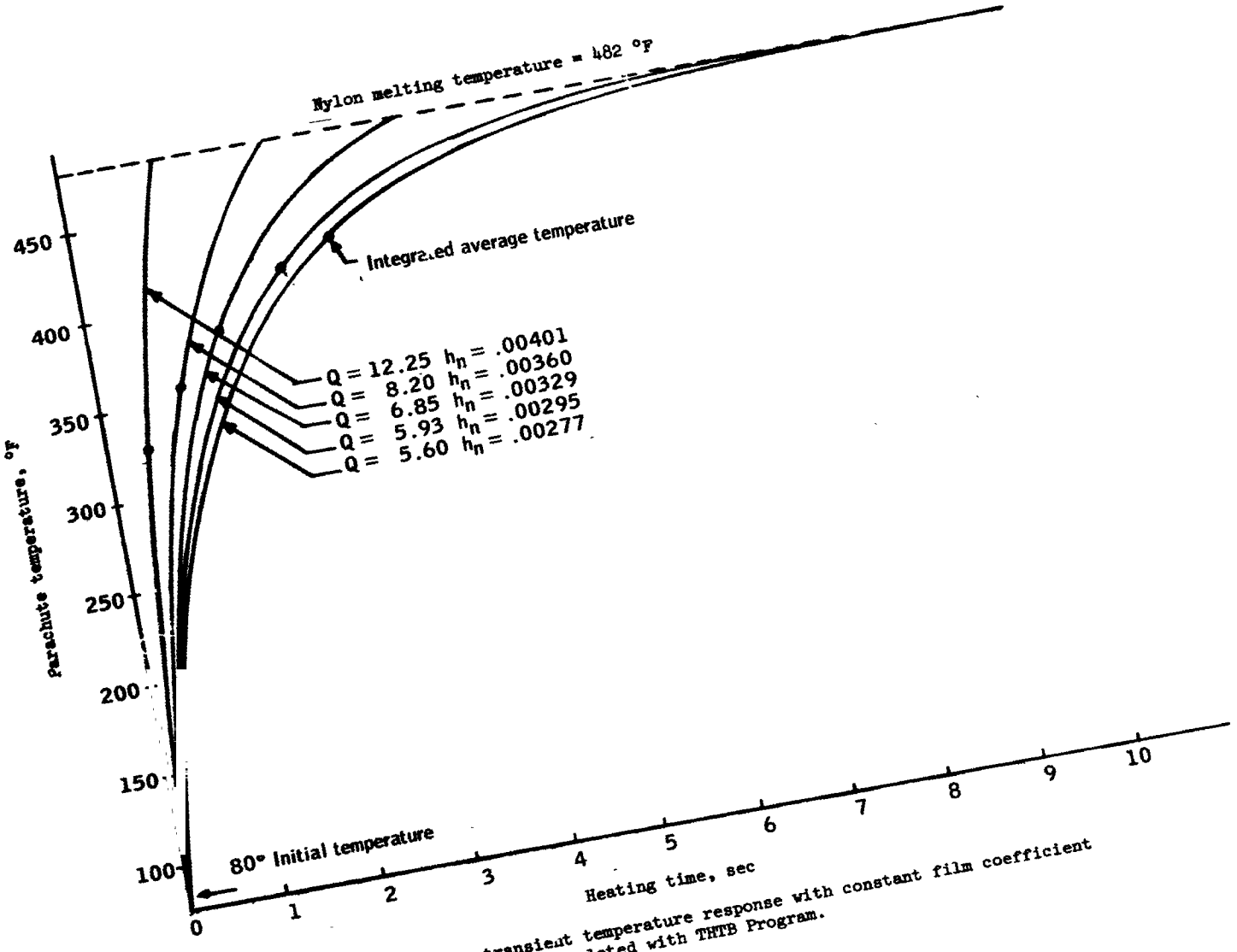

Figure 27.- Parachute transient temperature response with constant film coefficient calculated with THTB Program.

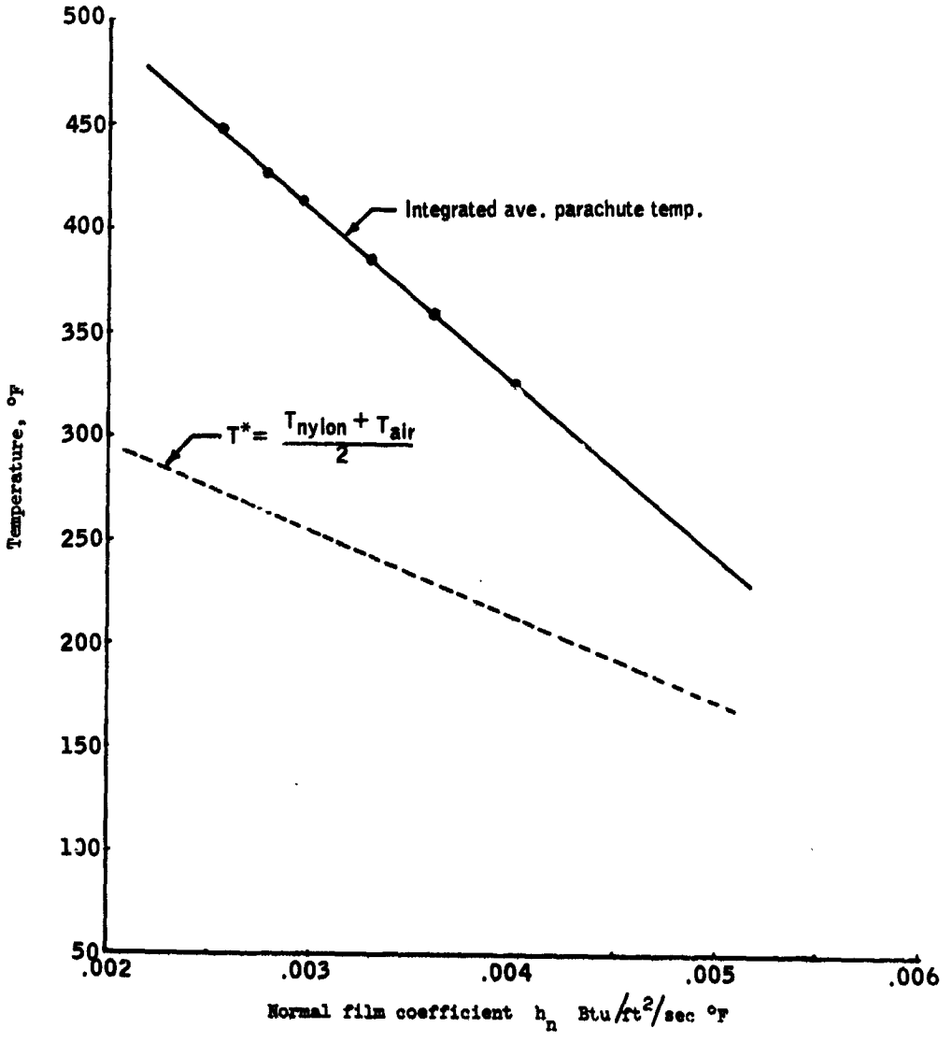

Figure 28.- Normal film coefficient as a function of temperature.

REFERENCES

1. Performance of and Design Criteria for Deployable Aerodynamic Decelerators. Technical Report No. ASD-TR-61-579, Dec. 1963.

2. Schoeck, P. A.; Hood, J. N.; and Eckert, E. R. G.: Experimental Studies for Determining Heat Transfer on the Ribbons of Fist Type Parachutes. WADC TN 59-345, Feb. 1960.

3. High, R. W.; and Fletcher, R. F.: Estimation of Fireball from Saturn Vehicles Following Failure on Launch Pad. NASA Program Apollo Working Paper No. 1181.

4. Thermal Radiation from Saturn Fireballs. TRW Report 2122-6001-T0000, vol. 1, Analysis, Dec. 15, 1965.

5. Thermal Radiation from Saturn Fireballs. TRW Report 2122-6001-T0000, vol. 2, Dec. 15, 1965.

6. Eldred, Charles: Stress Analysis of Apollo Main and Drogue Parachutes. TN in preparation NASA MSC.

7. Handbook of Thermophysical Properties of Solid Materials. Revised ed., Armour Research Foundation, 1961.